

Enhanced Visualization

for Improved Lesion Diagnosis in Virtual Colonoscopy

Erik Pols

TU Delft, October 2008

Acknowledgements

I would like to express my gratitude to all who have helped me to create this master thesis and to accomplish the research that preceded it. First and foremost I would like to thank my direct supervisors Frits Post and Charl Botha of the medical visualization group at the EWI faculty of the TU Delft. Their advice and extensive knowledge in the field of medical visualization proved indispensable. I also thank Lingxiao Zhao for his help to get me started and his adaptation of his curvature algorithm, and Simona Grigorescu and Vincent van Ravesteijn of the Physics faculty.

Furthermore I would like to thank Roel Truyen and Iwo Serlie attached to Philips Medical Systems who commented on my work and helped me wherever they could, as well as providing the financial and technical means to execute this research. I also thank Kees Visser for the technical support and Javier Bescos for his comments in the early phase of this research.

I also would like to thank Ayso de Vries and Marjolein Liedenbaum from the Amsterdam Medical Center who provided commentary from a clinical perspective and helped me to gain an understanding of the way radiologists think, something that is regularly undervalued. They also were my subjects in the expert evaluation for which I am thankful.

Last but not least I would like to thank my beloved fiancée for her never ending support, and my room mates for the late night in-depth discussions.

Erik Pols

Delft, October 2008

Contents

| | |
|---|----|
| Acknowledgements | 3 |
| 1. Introduction | 9 |
| 1.1. CT colonography | 9 |
| 1.2. Motivation | 9 |
| 1.3. Thesis structure | 10 |
| 2. Background | 11 |
| 2.1. Lesions | 11 |
| 2.1.1. <i>Polypoid lesions</i> | 11 |
| 2.1.2. <i>Flat lesions</i> | 12 |
| 2.2. Computed Tomography | 14 |
| 2.2.1. <i>The scanning process</i> | 15 |
| 2.2.2. <i>Data parameters and limitations</i> | 15 |
| 2.3. Volume ray tracing | 16 |
| 2.3.1. <i>Ray tracing</i> | 17 |
| 2.3.2. <i>The voxel traversal algorithm</i> | 17 |
| 2.3.3. <i>Iso-surface rendering</i> | 18 |
| 2.3.4. <i>Rendering the iso-surface</i> | 20 |
| 2.4. Advanced shading | 20 |
| 3. Previous work | 21 |
| 3.1. Polyp detection | 21 |

| | | |
|--------|--|----|
| 3.1.1. | <i>Spatial filtering</i> | 21 |
| 3.1.2. | <i>Shape indexes, curvedness and gradient concentration.</i> | 21 |
| 3.1.3. | <i>Polyp protrusion</i> | 23 |
| 3.1.4. | <i>Curvature streamlines</i> | 24 |
| 3.2. | Flat lesion detection | 24 |
| 3.3. | Colon wall visualization | 25 |
| 3.3.1. | <i>Unfolded cube</i> | 25 |
| 3.3.2. | <i>Flattened colon wall</i> | 25 |
| 3.3.3. | <i>Magic lens</i> | 26 |
| 3.3.4. | <i>Conclusion</i> | 26 |
| 4. | Research goals and quality criteria | 29 |
| 4.1. | Research goals | 29 |
| 4.1.1. | <i>Non-feature based enhancement</i> | 29 |
| 4.1.2. | <i>Feature based enhancement</i> | 30 |
| 4.2. | Quality criteria | 30 |
| 4.2.1. | <i>Object size</i> | 31 |
| 4.2.2. | <i>Usability</i> | 31 |
| 4.2.3. | <i>Technical criteria</i> | 31 |
| 4.2.4. | <i>Flat lesions and polyps</i> | 31 |
| 5. | Enhanced lighting, shadows and shading | 33 |
| 5.1. | Lighting models | 33 |
| 5.1.1. | <i>Point light</i> | 33 |
| 5.1.2. | <i>Directional light</i> | 34 |
| 5.1.3. | <i>Tube lighting</i> | 36 |
| 5.1.4. | <i>Three-point lighting</i> | 36 |

| | | |
|--------|--|----|
| 5.1.5. | <i>Rim lighting</i> | 39 |
| 5.1.6. | <i>Other lighting techniques</i> | 41 |
| 5.1.7. | <i>Subjective assessment</i> | 42 |
| 5.2. | Shadow models | 43 |
| 5.2.1. | <i>Shadows</i> | 43 |
| 5.2.2. | <i>Ambient occlusion</i> | 44 |
| 5.2.3. | <i>Subjective assessment</i> | 46 |
| 5.3. | Advanced shaders | 47 |
| 5.3.1. | <i>Threshold projection</i> | 47 |
| 5.3.2. | <i>Transparency</i> | 48 |
| 5.3.3. | <i>Transparency color mapping</i> | 49 |
| 5.3.4. | <i>Subjective assessment</i> | 49 |
| 5.4. | Conclusion | 49 |
| 6. | Feature dependent visualizations | 51 |
| 6.1. | Candidate visualization | 51 |
| 6.1.1. | <i>Realistic rendering</i> | 52 |
| 6.1.2. | <i>Meta color maps</i> | 53 |
| 6.2. | Curvature visualization | 53 |
| 6.3. | Wall thickness | 53 |
| 6.4. | Raised grey value level | 54 |
| 6.4.1. | <i>Transparency revisited</i> | 54 |
| 6.4.2. | <i>Flat lesion dilation</i> | 55 |
| 6.5. | Contrast fluid sticking to lesions | 58 |
| 6.5.1. | <i>Obtaining the small cluster contrast mask</i> | 58 |
| 6.6. | Conclusion | 60 |

| | | |
|--------|-------------------------------|----|
| 7. | Expert evaluation | 63 |
| 7.1. | Proposed techniques | 63 |
| 7.2. | Evaluation approach | 63 |
| 7.2.1. | <i>Reviewing speed</i> | 64 |
| 7.2.2. | <i>Lesions found</i> | 64 |
| 7.2.3. | <i>Esthetic value</i> | 64 |
| 7.3. | Results | 64 |
| 7.3.1. | <i>Rim lighting</i> | 64 |
| 7.3.2. | <i>Dilation</i> | 65 |
| 7.3.3. | <i>Dilation coloring</i> | 65 |
| 7.3.4. | <i>Contrast coloring</i> | 66 |
| 8. | Conclusions | 67 |
| 8.1. | The polypoid lesions | 67 |
| 8.2. | The flat lesions | 68 |
| 8.3. | Further research | 68 |
| 8.4. | Conclusion | 69 |
| | References | 70 |
| | Additional references | 73 |
| | Appendix A: Flat lesion index | 74 |

1. Introduction

The risk of developing colon cancer is strongly correlated with the appearance of polypoid lesions (also called polyps) in the large intestine [Santoro et al. 2008]. Not all polyps are dangerous; in fact only one percent of polyps smaller than one centimeter is dangerous. However, when polyps grow bigger the risk quickly increases to over fifty percent. Recently another kind of lesion was discovered that has a higher risk of developing towards cancer [Soetniko et al. 2008]. This so-called flat lesion is extremely hard to spot. Research in the past two years has made some effort to detect flat lesions automatically from CT scans but has yet been unsuccessful. This thesis tries to describe techniques that help radiologists spot polypoid and flat lesions in a CT Colonography by enhancing the rendered images of the colon interior surface wall.

1.1. CT colonography

Traditionally, when a doctor finds it necessary to inspect ones colon wall, the examination is executed by inserting a fiber optic camera or a CCD camera into the colon. This usually is a painful process for the patient if applied without sedation.

CT colonography, or virtual colonography tries to provide an alternative. Computed tomography (CT) is a non-invasive method that generates 3-dimensional images of the human body. If the patient has been prepared correctly, a representation of the colon wall can be constructed from these images. A radiologist can then examine the colon wall by moving through the colon with a virtual camera. In spite of the obvious advantages of colonography over colonoscopy, the technique is not yet in widespread use. This is mainly due to the limited level of information in a CT scan. For example, it is not possible to see the structure, color and wetness of the colon wall, factors that help a reviewer find malignant tissue [Cotton et al. 2004].

1.2. Motivation

After the CT scan is performed, the colon wall is reconstructed from the scan using iso-surface rendering. An iso-surface describes a surface through constant intensities in the voxel data. This iso-surface is

then rendered on a screen using volume rendering. Until now, a simple single color map was used with a single light source at the location of the camera. All information under the surface is discarded during the iso-surface rendering process, making it only available by directly looking at the slices. The goal of this thesis is to provide enhancement methods that increase the number of found polypoid and flat lesions during a colon review.

Our attempts towards this are twofold in focus. Firstly, we try to enhance the existing visualization without increasing the amount of visualized information but merely shifting the focus of that information. Secondly, we look at techniques that may increase the amount of information visualized thus giving the radiologist a better idea of what he is looking at. Our problem formulation is therefore twofold:

How can a colon visualization be enhanced so that more relevant information will be perceived by the radiologist while keeping the amount of displayed information the same?

Can the visualization of extra information about the colon wall shape or other features help the radiologist develop a better understanding of the structure of the colon wall resulting in more found lesions?

1.3. Thesis structure

This thesis is roughly divided in two sections. After the theoretical background which provides necessary mathematical and factual foundation on which the rest of the thesis relies, and the previous work, we will first focus on non-feature dependent techniques. Different lighting models are examined and the use of advanced shadow techniques is discussed. Also, the use of transparency is discussed. After that, we turn to the second part, which tries to enhance the visualization by focusing on specific features of lesions. This part will rely heavily on research in the field of automatic lesion detection. The wrap up will consist of results of the user test evaluation and the conclusion.

2. Background

Before we can elaborate on the problem of this thesis and some proposed solutions, some additional knowledge is required. Although the perspective of this document is primarily from a technical point of view, we would like to dedicate a small part to the clinical perspective to give the reader an idea what it is we are after and why it is important. Next, a short introduction to the CT scanning process will be given. After that, the ray casting algorithm will be explained, which will be the main platform for most of our experiments.

2.1. Lesions

Lesions are extraordinary growths of tissue [Stryker et al. 1987]. Colon lesions grow in the large intestine, which is the last part of the digestive system. Most lesions are not cancerous, or benign. However, over time, some lesions can become malignant, which is why doctors remove all lesions when they find them. Most lesions don't cause any symptoms, which is why they usually are found during regular checks or while the patient is being tested for something else. Despite their usually harmless characteristics, colon cancer is the second leading cause of death through cancer in the United States [Giardiello 2008].

Lesions can be divided into two categories which differ not substantially from a clinical point of view, but require a different approach when trying to detect or visualize them. Both will be discussed next.

2.1.1. *Polypoid lesions*

Polypoid lesions are lesions that usually grow on a stalk or protrude substantially from the colon wall (figure 2.1). Polypoid lesions or polyps have been known for quite a while, and are very common. Some studies estimate that 50% of people over the age of 60 harbor at least one polyp [Santoro, M. et al. 2008]. The process of a polyp becoming malignant is a slow process, usually taking up to 10 years. Although everyone can develop malignant polyps, there are several factors that increase the chance of a polyp being malignant.

Several kinds of polyps are believed to exist [Giardiello et al. 1995]. 90% of all polyps are hyperplastic polyps which is the benign kind. The clinical value of this kind of polyps was long considered insignificant, they are now recognized to possess some malignant potential [Morimoto et al. 2002]. Polyps

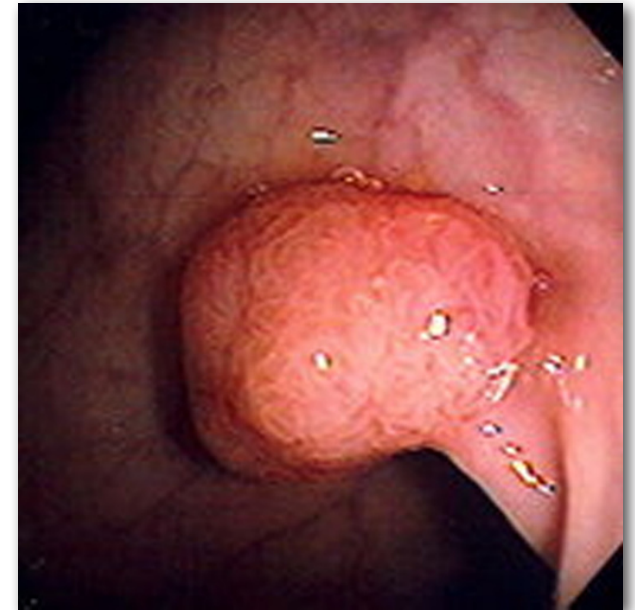


Figure 2.1 Polypoid lesion [Bamboo G. 2006]

that have a much higher potential of becoming cancerous are called adenomatous polyps or adenomas. Polyps can have different histologies (microscopic anatomy) [Giardiello et al. 1995]. Several histologies exist, namely tubular, tubulovillous and villous. Their difference is mainly found in the cellular structure of the polyp. Tubular adenomas have a tube-like structure. This is the most common form. Villous adenomas have a ruffled structure and are the least common but meanwhile also the most harmful. Tubulovillous adenomas are a mix between the two. Unfortunately there is no way of distinguishing between hyperplastic and adenomatous polyps or between their histologies without examining them under a microscope, which is why doctors usually remove them all during an optical colonoscopy. This latter process is called polypectomy and is usually performed by placing a noose or snare around the base of the polyp and cutting through the base [Charette 2008].

A second factor that increases the chance of a polyp becoming malignant is its size. The larger a polyp grows, the more likely it is to become cancerous. Polyps smaller than 1 cm have a chance of less than 1% of becoming cancer, but once the polyp grows larger than 2 cm the chance increases to 20%.

Polyps are detected during a virtual or an optical colonoscopy. In the latter case, the polyps can be removed instantly. In case a virtual colonoscopy is performed and polyps are detected, a follow-up optical colonoscopy is required.

2.1.2. Flat lesions

A different type of lesion was discovered a few years ago, called a non-polypoid colorectal neoplasm, or a flat lesion [Kudo et al. 2000]. Doctors were skeptical for a long time about the question whether flat lesions exist at all. However, some studies showed that flat lesions existed in Japan, and later studies proved them to exist in other parts of the world as well. A recent study in a California hospital by Soetniko et al. where 1819 patients that were both symptomatic and asymptomatic were examined proved that the prevalence of flat lesions in this target group is 9.35%. Moreover, this study showed that they are five times more likely to develop cancer than polyps, even after correcting for the polyp size [Soetniko et al. 2008].

Flat lesions are usually overlooked during colon cancer screening because of their size and their structure which often closely resembles healthy colon wall tissue (figure 2.2). A major difference with polypoid lesions is that their size does not affect the chance of them being cancerous. The structure of flat lesions is the same as that of polypoid lesions.

Which features describe a flat lesion best is a question that has not yet been answered. Because almost no research has been performed in this research area, for our research we were forced to try a lot of potential features ourselves. There are four features that possibly describe the flat lesions.

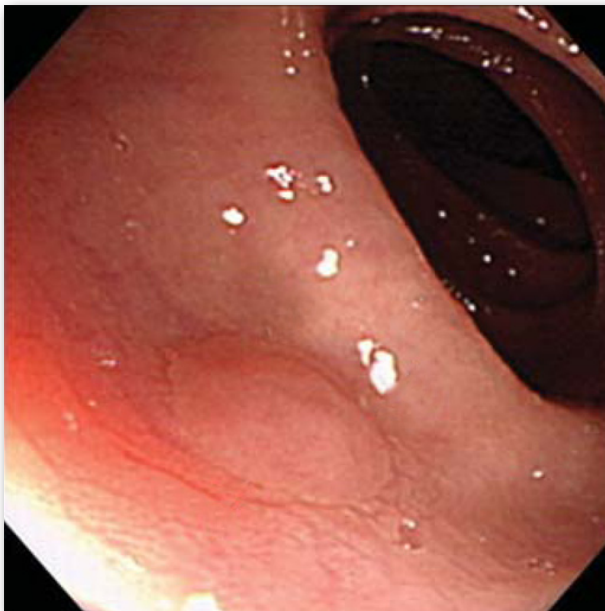


Figure 2.2 Flat lesion [Park 2006]

An anomalous deformation of the colon wall surface

Although usually a deformation of the colon wall is visible, the deformation is not well defined like the deformation of polypoid lesions. The most general classification of lesions that can be made is illustrated in figure 2.3.

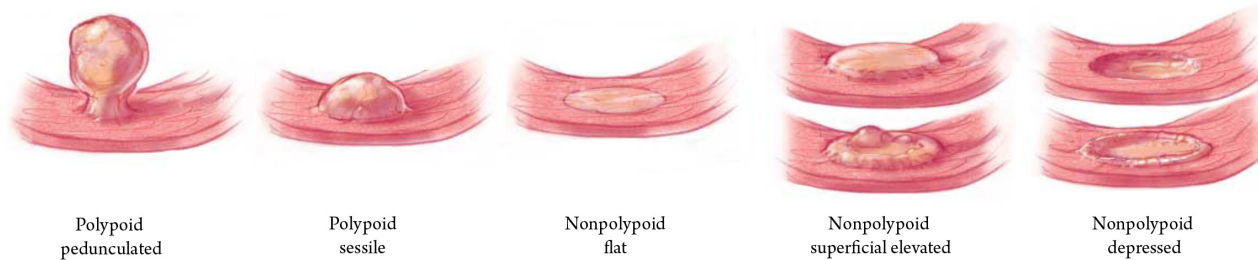


Figure 2.3 Lesion types. [Soetniko et al. 2008] Image copied with permission from Soetniko.

Flat lesions are usually defined as one of the last three cases. All kinds of combinations can exist. Also, flat lesions do not have to have a circular shape. They can grow parallel to the wall but also in folds, thereby thickening the fold.

A thickened colon wall

The tissue in the wall is likely to thicken the colon wall. Therefore, the thickness of the colon wall is argued to be a possible feature of flat lesions by radiologists and researchers from the Amsterdam Medical Center we spoke to.

A raised HU level inside the flat lesion

Most researchers agree that the anomalous tissue formed by the colon wall has a slightly raised HU level value. The raised value ranges between 30 and 40 HU values. Unfortunately the lesion is usually surrounded by blood, stool and other non-wall tissue that all have HU values in the same range. It is unsure whether this feature will be distinctive enough in order to find the flat lesions. In fact, Neri found that there were no differences in mean attenuation values between stool, polyps and cancer [Neri et al. 2005].

Contrast fluid adhering to the colon wall surface

Depending of the structure of flat lesions, contrast fluid might have a tendency to stick to the lesion surface. O'Connor investigated this and found that contrast sticks to 77% of the researched lesions with a villous histology against 43% of the ones with a tubular histology [O'Connor et al. 2006]. Hyperplastic lesions also have a probability of 44% that contrast fluid adheres to them. The difference between the rates for the tubular and villous histology can probably be explained by the ruffled nature

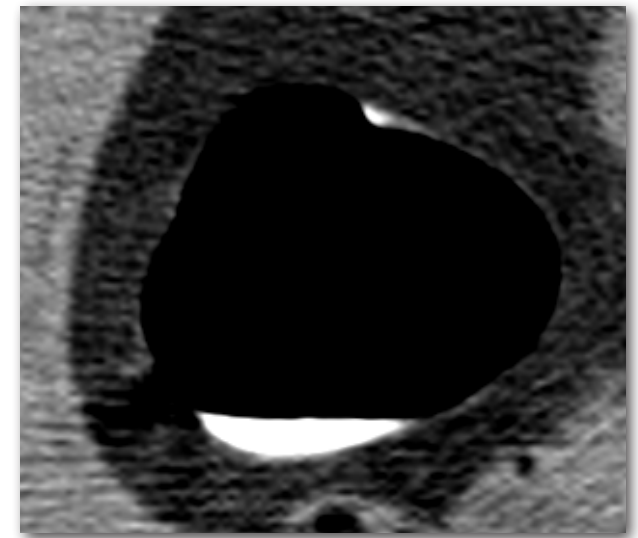


Figure 2.4 Flat lesion with adhering contrast fluid

of the villous histology. Neri reports an average increase of 80 HU tested on 28 cases [Neri et al. 2005] which is consistent with our findings (Appendix A).

While the detection of polyps in colon scans is fairly successful, attempts to detect flat lesions have been largely unsuccessful so far.

The lack of good features translates itself into the ratio of found lesions in CT data sets. Experts we spoke to estimate that only 25% of all flat lesions is found when using only the CT scan. Usually the flat lesions are found with optical colonoscopy, and later matched against the CT scan. It occurs often that flat lesions cannot be located in the data set or that the confidence level is very low. According to the expert, the fact that the ratio is that low lies not in the fact that the information is not visible, but simply because the information is not there.

2.2. Computed Tomography

Computed Tomography, also known as Computed Axial Tomography (CAT), is a medical imaging technique that uses tomography which means imaging by sections [Hawkes 2008]. By rotating an X-ray tube (also called the gantry) projections from a large number of directions can be computed (figure 2.5) which can be combined into a 2D slice of the body using the mathematical procedures known as tomographic reconstruction. Repeating this for a number of times at equally spaced distances along the body results in a 3D representation of the body. The values in this representation are called attenuation values (named after the attenuation of the ray energy when it perpetrates an object)

Whether CT Colonography is viable for screening patients for either flat or polypoid lesions is a question that has been discussed in the literature. Pickhardt claims in a study performed on 600 patients where 827 lesions were found that CT Colonography is not yet ready for widespread clinical application [Pickhardt et al. 2003]. According to his study, CT Colonography had a sensitivity of 39% for lesions sized 6 mm or more and 55% for lesions sized larger than 10 mm, which is considerably lower than conventional colonoscopy results, which had a sensitivity of over 99%. He also claimed that participants expressed no clear preference for either technique. Cotton, on the other hand claims that CT Colonography compares favorably with optical colonoscopy in terms of detection [Cotton et al. 2004]. He performed his studies on 1233 asymptomatic adults and claims sensitivities of 93.9% for lesions of 8 mm and larger and 88.7% for lesions of 6 mm and larger whereas optical colonoscopy sensitivity values were 96% and 79.6% respectively.

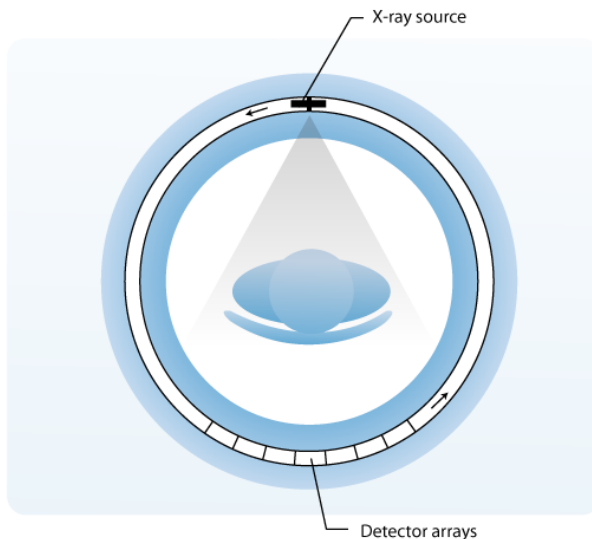


Figure 2.5 Computed Tomography

Another study was published at the time of writing of this thesis, which was executed under 2600 participants of 50 years and older [Johnson et al. 2008]. This study showed that CT Colonography was able to identify 90% of the lesions of size 10mm and larger that were identified with colonoscopy. For lesions sized 6mm and up the sensitivity was 78%.

2.2.1. *The scanning process*

Although Virtual Colonoscopy is a noninvasive technique, some preparations need to be taken nevertheless [Waye et al. 2003]. The patient is advised to take a low-fat and low-fiber diet a few days prior to the examination and often some contrast fluid is ingested by the patient in order to tag remaining stool. For tagging, a substance called iodine or dilute barium is used which makes the residuals appear white on the scan. Once the patient has been prepared, the examination is ready to be performed. Prior to the examination, the colon is insufflated with either room air or carbon dioxide. Next, the CT Colonography is performed first in the supine position and secondly in the prone position. This is required in order for the areas that were formerly covered in fluid to be visible.

After the scan, a radiologist will examine the data. Whether he will directly use the orthogonal slices (figure 2.6) or the 3D reconstruction of the colon is a matter of personal choice. A typical workflow is to closely follow the colon in the orthogonal views. When a radiologists finds something suspicious, he inspects the corresponding location in the 3D view to get a clearer idea of the deformation on the colon wall.

2.2.2. *Data parameters and limitations*

CT technology is subject to heavy research and has improved a lot over the past years. A typical data slice consists of 512 x 512 pixels. The amount of slices per data set ranges between 256 and 1000 slices, although more is certainly possible. The distance the scanner moves between each slice is called the pitch and determines the axial resolution of the data set in the direction of the scanning process. A data set is called isotropic if the spacing in all axial directions is equal, e.g. the voxels in the data set are cubed. Usually this is not the case, which is when a data set is called anisotropic. This implies that this must be compensated for when rendered in order to ensure correct proportions.

Attenuation values (or data values) are measured in Hounsfield units (HU), named after Sir Godfrey Hounsfield who co-developed the first CT scanner in 1972. Figure 2.7 shows a scale that displays typical CT values found in CT data.



Figure 2.6 Prone view of the pelvis area. The black areas represent the colon lumen

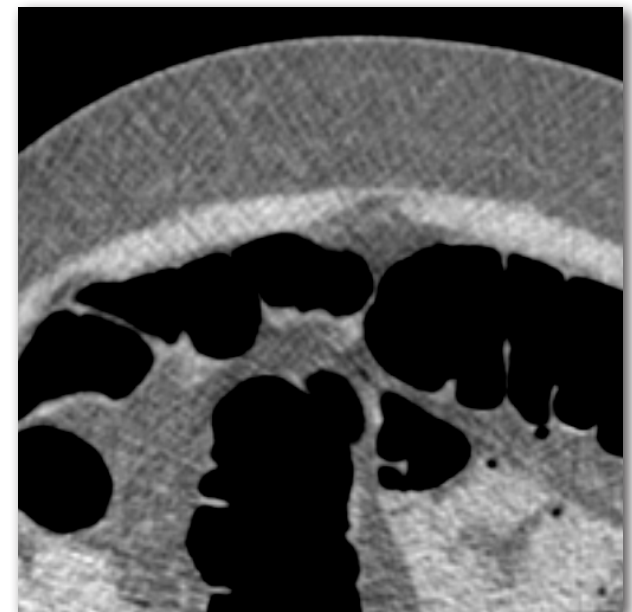


Figure 2.8 Noise distorting the area near the colon wall

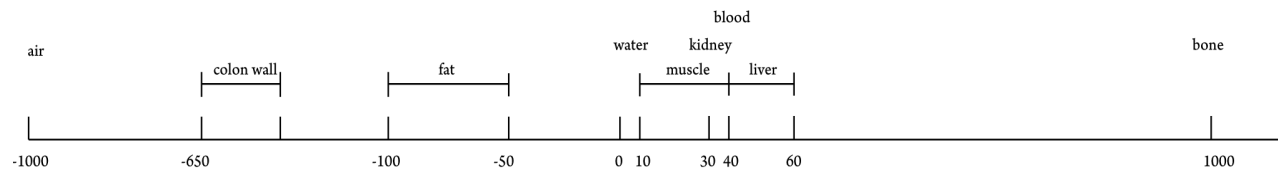


Figure 2.7. Hounsfield unit scale [Medyclopaedia 2008]

Usually the data set is stored in grey values which are converted to HU values when needed. These grey values can be stored in two bytes ($0 - 2^{16}$), which results for a data set with 800 slices in a size of 400 MB. Being able to host multiple data sets in memory therefore still requires powerful hardware.

CT data quality suffers considerably from noise produced by the CT scanner (figure 2.8). The amount of noise that is generated can be reduced by increasing the radiation dose emitted by the scanner, however, this can induce cancer in the exposed individual after a latent period. The noise in a CT data set can be modeled with a zero-mean Gaussian filter with a variable noise variance [Serlie 2007]. This variance is variable over the image plane but is also dependent on structures in the body with high HU values, like bone. Therefore, usually the noise in a CT data set is modeled as white noise. Serlie showed that near the edge of the colon, a Gaussian can be used to reduce the noise. We cannot assume this to be true for areas behind the colon wall, therefore we will use both mean and Gaussian filters in our tests.

Although the transition of lumen to colon wall does not suffer extensively from noise because the difference in HU values between the lumen and the wall tissue is relatively large, the area behind the wall and thus the area where polyps reside consists mostly of tissue, blood and fat, values of which are ranked fairly closely together, making them very hard to distinguish. Attempts have been made to reduce this noise, but unfortunately most of them also result in a loss of effective resolution. Schaap proposes a noise reduction technique that is based on a group of techniques called anisotropic diffusion [Schaap et al. 2008]. This technique tries to reduce noise while preserving edges. Schaap reports excellent results with a high performance implementation. Unfortunately this paper was published after it could be of use to us but is recommended for use in future research.

2.3. Volume ray tracing

After the 3D data set has been acquired it can be visualized in a number of ways. Due to limitations in computer speed, for a long time radiologists looked directly at the slices produced by the scanning device. Although usually effective, it is generally quite hard to infer 3D information from the slices.

Therefore, attempts were made to render the data in 3D. Ray tracing has become the main algorithm of choice for generating 3D volume images.

2.3.1. Ray tracing

In our environment, light that is emitted by light sources like the sun or artificial lights usually bounces off objects and surfaces into our eyes, which gives us the ability to experience color, shape and intensity. Ray tracing tries to mimic this behavior in a backwards manner by casting rays from a camera location into the scene (Figure 2.9). Each ray must be tested against all object in the scene to find out which object is the first object the ray intersects with. Using the material and light properties, a color representation can be generated that is rendered on the original pixel location.

In its most basic form, the ray tracing algorithm is a powerful but slow method. There are several ways to increase the performance without the use of parallel CPU architectures. The first is the use of hierarchical bounding volumes, which aims to encapsulate complex objects in a much simpler bounding object. When tracing a ray, the ray is tested against just the bounding box. When the ray hits the box, the ray is tested against the individual components of the object. The second method is the use of space partitioning, which is a technique that is directly applicable to volume ray tracing. Amanatides and Woo have described a very efficient method to do this.

2.3.2. The voxel traversal algorithm

The algorithm presented by Amanatides has become the standard in volume ray tracing because of its simplicity and high performance [Amanatides et al. 1987]. The algorithm consists of two phases: initialization and traversal. During initialization, the starting voxel is determined. Also the ray is defined as:

$$\vec{u} + t \cdot \vec{v}, t \geq 0$$

If outside the grid, the ray is advanced to the point where the ray enters the grid. At the same time, two variables named tMaxX and tMaxY are initialized, which represent the value of t at which the ray crosses the first horizontal respectively vertical voxel boundary. Finally, tDeltaX and tDeltaY are computed. tDeltaX indicates how far along the ray we must move in (units of) for the horizontal component of such a movement to equal the width of a voxel. Similarly, in tDeltaY indicates this length for the horizontal component.

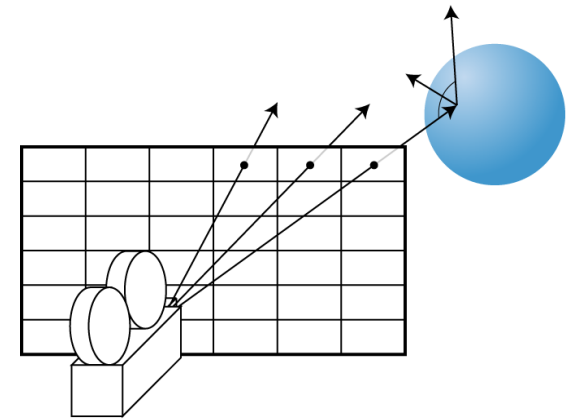


Figure 2.9 Ray tracing

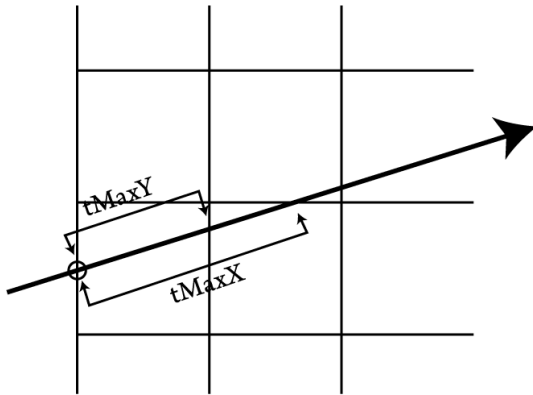


Figure 2.10 The maximum length to travel before hitting a boundary

After initialization, the traversal can start. This traversal can best be explained with pseudo-code and an illustration (figure 2.10)

```

loop {
  if(tMaxX < tMaxY) {
    tMaxX= tMaxX + tDeltaX;
    X= X + stepX;
  }else {
    tMaxY= tMaxY + tDeltaY;
    Y= Y + stepY;
  }
  NextVoxel (X, Y);
}

```

In words, the algorithm continually compares how far the next horizontal and vertical crossings are away by keeping track of these crossing points in units of t . If the vertical boundary is closer, $tDeltaX$ is added to $tMaxX$ until it is not closer anymore and vice versa. The exact location of the crossings is not calculated, but this can easily be done by entering the value into the aforementioned formula.

In Armanatides algorithm, the loop continues until a hit is found or the ray exits the boundary volume. In volume ray tracing, the condition can be a number of things [Levoy 1988]. A popular method is Maximum Intensity Projection, where the maximum intensity found in the voxels that the ray crosses is projected on the corresponding pixel on the screen. A second popular method is Direct Volume Rendering, which is a range of techniques based on the fact that an opacity value and a color value is associated to grey values. Both techniques usually suffer from a high amount of fuzziness. The technique most algorithms in this thesis are based on however is iso-surface rendering, which usually generates much sharper images. Iso-surface rendering generates results comparable with DVR when applying high opacity values for grey values higher than the iso-surface value, and fully transparent values for grey values lower than the iso-surface value.

2.3.3. Iso-surface rendering

An iso-surface (figure 2.11) is the surface in a continuous field at which the value equals a pre-defined iso-value [Bosma 2000]. Because a volume data set is not continuous, an approximation of the iso-surface needs to be calculated. Bescós describes numerous ways to calculate this iso-surface while traversing the volume data set using Amanatides algorithm [Bescós 2003]. It would take us too far off track to give an in-depth discussion of all methods. Instead we give a birds-eye view of the most popular methods. For a detailed discussion we refer the reader to [Bescós 2003].

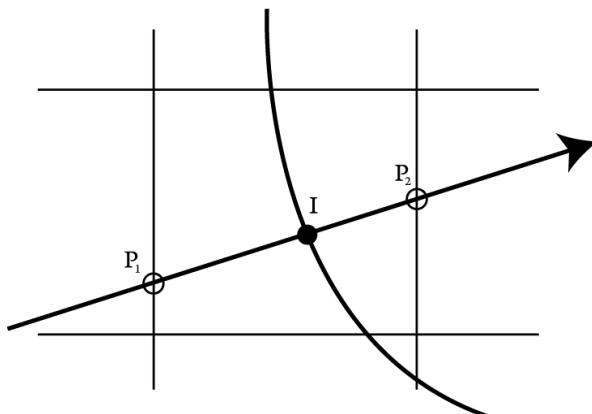


Figure 2.11 A ray intersecting an iso-surface

Marching Cubes

Marching Cubes is a widely used algorithm for reconstructing iso-surfaces. The surface is approximated by a polygon mesh that is generated from the data set. For every cell in the data set, each of the corresponding 8 voxels is compared with the iso value and classified as above or below. This results in possible configurations which can be reduced to 15 cases by symmetry. A few examples are shown in figure 2.12.

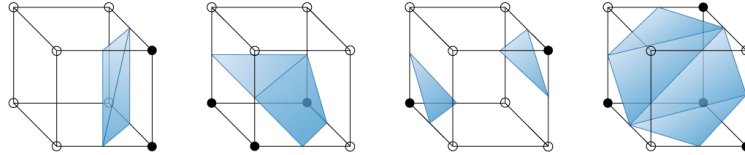


Fig 2.12 Four possible marching cubes configurations

Based on the configuration, up to 4 triangles are added to the mesh in such a way that one side of the surface contains values higher than the iso value and the other side values lower than the iso value. Once the mesh is constructed, it can be visualized using either rasterization or ray tracing.

Direct Volume Rendering

Another way to approximate the iso-surface is to use an adapted version of Direct Volume Rendering. By taking a step function for the opacity function that is 0 for values below the chosen iso value and 1 for values higher than the chosen iso value, the surface can be visualized. To ensure a high level of detail that does not show aliasing, it is necessary to re-sample the data set with a trilinear interpolator at equidistant steps along the ray. When the segment where the iso-surface is crossing the ray is found, the location is estimated to be exactly between the two segment end points.

Iso-surface Volume Rendering

Iso-surface Volume Rendering is an iterative algorithm that computes the iso-surface numerically. The algorithm consists of two parts. If the cell is a cell that contains the iso-surface, a point is inserted exactly between the points where the ray enters and leaves the cell. The two resulting segments are evaluated and the first segment that intersects the iso-surface (e.g. one point is higher than the iso value and the other is smaller) is selected. This is repeated for a number of iterations.

After this, the second step is executed which is the approximation of the location of the intersection of the ray and the iso surface using a Regula Falsi iteration. This results in the final approximation of the iso-surface location.

All methods described can produce a high level of accuracy when the parameters of the algorithms are adjusted accordingly. However, Bescós showed that the Iso-surface volume rendering method required the least amount of computation for a given spatial error value. This method is also the method that we will use in our tests.

2.3.4. Rendering the iso-surface

When the approximated location of the iso-surface has been determined, the color of the final pixel can be determined using the surface material properties and the light properties. Usually, these properties consist of an ambient, a diffuse and a specular component. These properties are combined in the Phong reflection model which is described as follows. We include it here because it is a starting point for a number of our techniques:

$$I = k_a I_a + \sum_{i=1}^n I_{li} [k_d (N \cdot L_i) + k_s (N \cdot H_i)^{n_s}]$$

where I is the final intensity of the surface and I_a the ambient term. k represent the material attributes that are defined for a type of surface. The equation sums over all lights n in the scene. L_i defines the vector pointing at the light i , and N is the normal vector of the surface. L defines the direction vector to the light and lastly H_i is the average between L and V (also called the halfway vector), where V is the viewing vector. The halfway vector is useful for calculating the specular reflection, which is dependent on the viewing direction. We could also use the dot product between the viewing vector and the reflection vector but by using the halfway vector this term can be treated as a constant when the location of both the light and the viewer is at infinity. See figure 2.13 for a graphical explanation. The Phong implementation will be used as a basis in most of our tests. A graphical example can be found in figure 2.14.

2.4. Advanced shading

The Phong model can be extended in numerous ways to add additional levels of realism. Color can be added to the equation by replacing the constants k with an RGB vector. Transparency can be achieved by defining an opacity value for the surface, and multiplying the result of the rendering equation with this value before continuing the original ray trace. This process can be repeated for every surface that is hit. For volume ray tracing algorithms it is necessary to carefully define how the grey values are transformed to opacity values. This can be achieved using a transfer function.

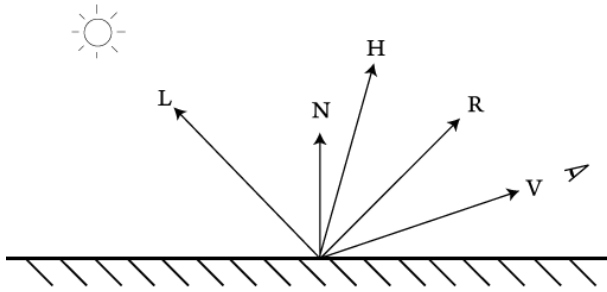


Figure 2.13 The phong reflection model



Figure 2.14 Iso-surface rendering of the spine

3. Previous work

Since volume rendering in medical imaging gained more acceptance, the research towards detection of lesions increased as well. With a polyp detection rate of about 90% of the amount of polyps found with optical colonoscopy, the detection rate in polyp detection is nowadays almost as high as the rate with visual inspection [Johnson 2008]. However, the research towards detection of flat lesions did not make that much progress yet, both because the field of research is relatively new and because the flat lesion detection problem is much harder. Because detection and visualization are closely related fields, previous work on detection of lesions and visualization will be evaluated.

3.1. Polyp detection

Detecting polyps has been attempted in a variety of ways, four of which we will examine in more detail.

3.1.1. *Spatial filtering*

One of the first to attempt automatic [Summers 2000] detection of polyps in CT scans was Summers et al. He based his method on a spatial filtering technique applied to synthetically placed polyps. The primary shape criterion is elliptic curvature shaped like a peak, which targets areas that protrude inward from the wall of the colon and are circular. The used kernel was 5x5x5. A spatial filtering alone did not eliminate enough false positives, which Summers tried to enhance by also taking a typical polyp size of 10mm into account as well as geometric features like mean curvature and principal curvatures. These parameters make Summers method sensitive to deviations in size and curvature. He reports sensitivities of 60%. An example can be seen in figure 3.1

3.1.2. *Shape indexes, curvedness and gradient concentration.*

Yoshida continued the idea of detection based on geometric features [Yoshida 2002]. First, the colon wall is extracted to improve render speed and reduce false positives. In this two-step process, the rough outline of the colon wall is first extracted based on a-priori anatomical knowledge. The air surrounding the body area, the spine, pelvis and ribs and the lung basis are removed by thresholding the volume which he assumed to be isotropic. This thresholding is followed by a connected component analysis which yields the contiguous regions that correspond to extracolonic structures. These structures are dilated to make sure they are fully removed. Because the resulting extracted colon mask may still con-

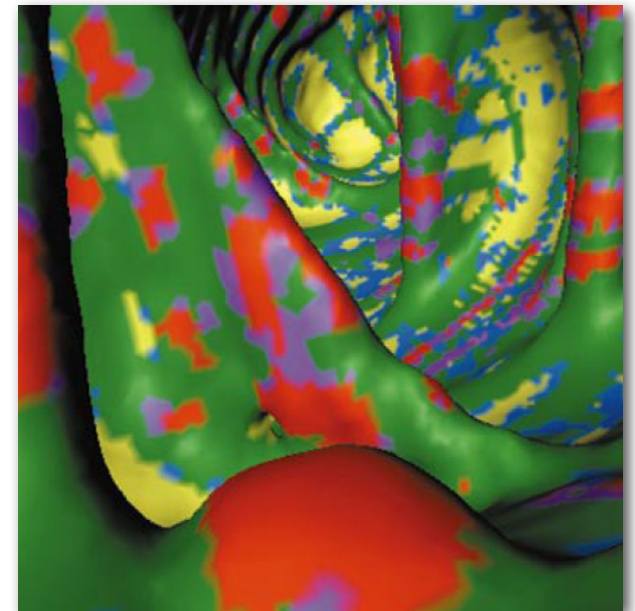


Figure 3.1 Areas that match Summers algorithm are colored red [Summers 2000]

tain the small bowel and stomach that adhere to the colon wall, a second step is executed. This second step consists of placing automatically selected seed points in the colon mask, and another segmentation with the resulting dilated lumen. The main advantage of this method over surface reconstruction is the fact that the complete lesions remain in the segmentation as opposed to just the description of their surface.

After the colon mask has been retrieved, polyps are detected based on geometric features. Polyps appear as relatively small, cap-like structures, whereas the colon wall tends to appear as nearly flat with a lot of ridge-like folds. To characterize these features Yoshima proposes to use a combination of the volumetric shape index and the volumetric curvedness.

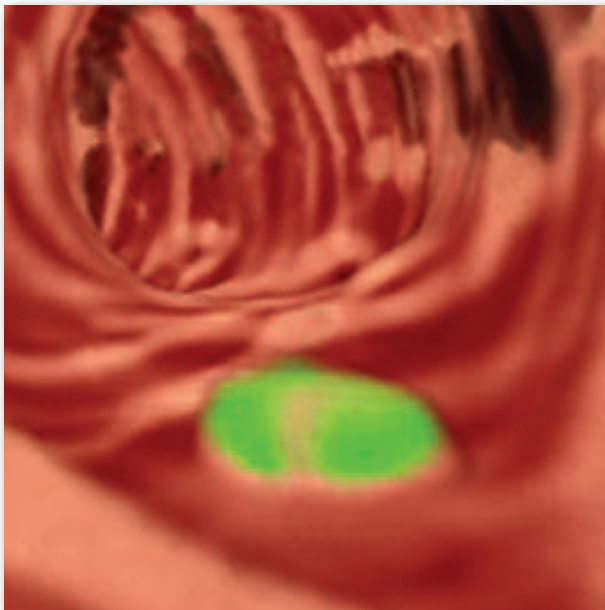


Figure 3.4 A polyp that matches Yoshimas parameters [Yoshida 2002]

The volumetric shape index is an index ranging from 0 - 1 and can be defined for every point in a volume. Five base shapes are defined as cup, rut, saddle, ridge and cap, evenly distance spaced in the 0 - 1 range. Intermediate shapes are also defined, so for example an index of 0.8 is the transition from ridge to cap.

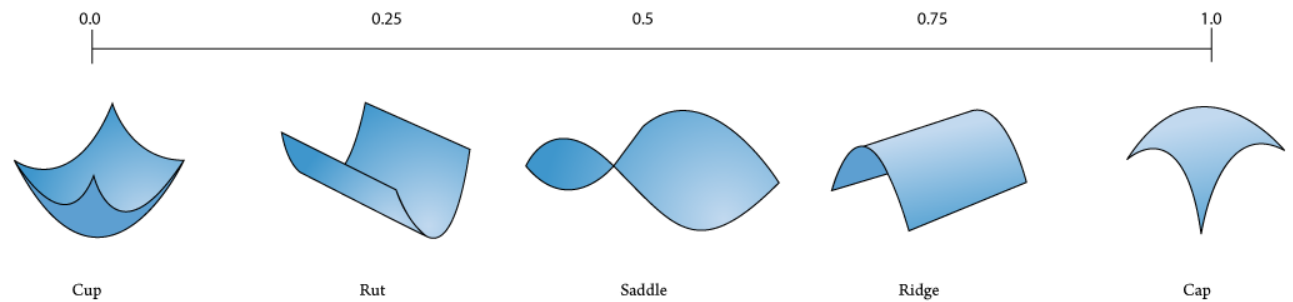


Figure 3.2 Surface shape indexes.

Volumetric curvedness on the other hand defines how gently the previously described shape is curved and is defined in terms of the magnitude of the effective curvature on the surface. It ranges from negative infinity to positive infinity. Curvedness also defines size information; a very subtle shape change is defined by a very low curvedness whereas a large positive value defines a sharp edge.

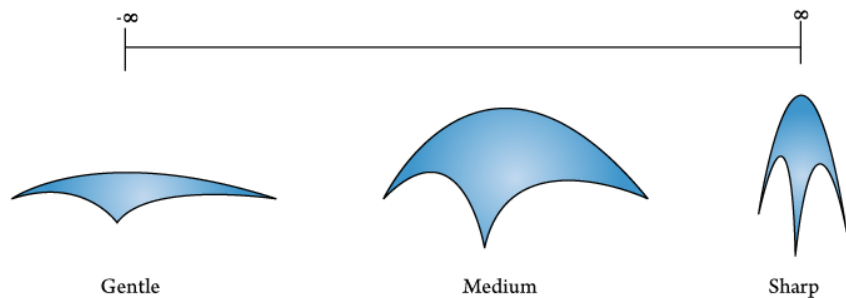


Figure 3.3 Surface curvedness

Yoshida reports optimal results with shape indexes between 0.9 and 1.0 and curvedness values between 5.0 and 12.5 [Yoshida 2002]. A fuzzy c-means clustering algorithm merges multiple selections of the same polyp. To further reduce false positives, a feature called Gradient direction concentration (GDC) is introduced, which is a measure for how much of the surrounding gradient vectors are pointing towards the given point. This feature is extracted by evaluating all voxels in the vicinity of a given voxel. The more vectors are pointing towards the voxel, the higher the GDC. According to Yoshida, this can be used effectively to distinguish between polyps and stool. Statistical classifiers are used to determine the final selection. Yoshida reports similar results as when a colon is screened by radiologists.

3.1.3. Polyp protrudedness

Another method is proposed by Van Wijk et al. and exploits the fact that the deformation caused by polyps have a second principal curvature that is larger than zero [Van Wijk et al. 2006]. This means that only surfaces that curve in two directions are affected and not surfaces that are curved in one direction. An example of the latter is a fold, which remains unaffected. Van Wijk bases his method on a triangle mesh generated with the Marching Cubes algorithm. When the second principal curvature is larger than a predefined threshold at a vertex, the surface is flattened until it falls below this threshold (figure 3.5). The deformation is executed using an iterative diffusion algorithm that was originally designed to reduce noise. Van Wijk modified this algorithm so that it deforms the surface based on the second principal curvature. The protrudedness is then defined as the difference in height between the deformed and original surface.

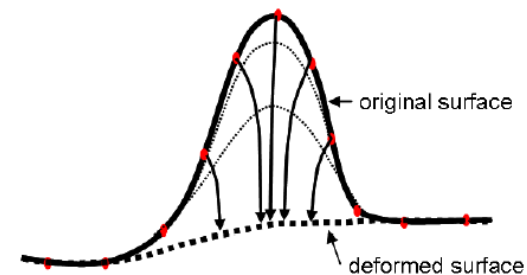


Figure 3.5 Flattening a polyp

Results are evaluated using a study of 249 asymptomatic patients who all underwent both a colonoscopy and a subsequent CT scan. Van Wijk reports a sensitivity of 95% with approximately 10 false positives per data set.

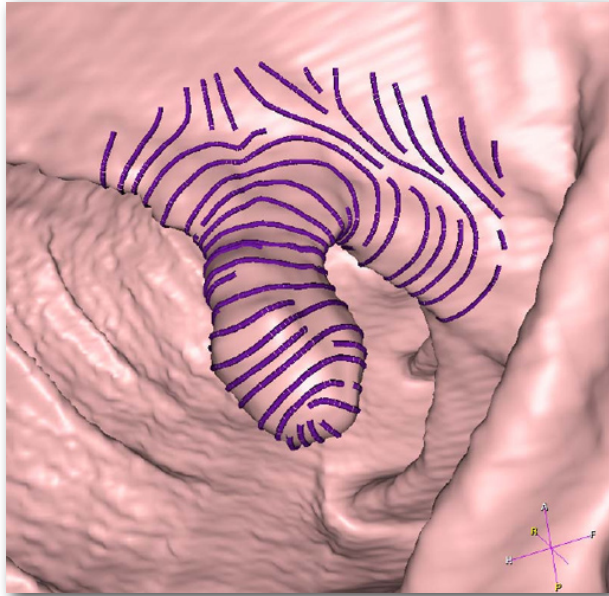


Figure 3.6 Curvature streamlines [Zhao 2006]

3.1.4. Curvature streamlines

A third technique is presented by Zhao et al. and detects polyps by selecting curvature streamlines that describe the neck area of polyp candidates [Zhao 2006]. Although closely related to both the work of Summers and Yoshida, this technique takes the interpretation of the curvature one step further than other techniques. Although Zhao's method is applicable to both implicit iso-surfaces and triangle meshed, the method described here is applicable to implicit iso-surfaces.

The principal curvatures are estimated in a three-step algorithm. It would be out of the scope of this thesis to describe this process in detail, a birds eye overview will be given instead. After determining the principal curvature directions, the curvature streamlines are generated. The last step clusters them.

Firstly, the principal curvature directions are determined for all points on the iso-surface. This is done by calculating the gradient vector and the Hessian matrix. One axis of the Hessian matrix is aligned with the gradient vector. On the resulting matrix an eigen analysis is performed, and the resulting eigen vectors correspond to the principal directions in the tangent plane at the point on the surface.

Next, seed points for curvature streamlines are selected on the surface, and the streamlines are generated by following the principal curvature direction calculated in the previous step in both curvature directions in a stepwise manner. Every step will usually end up away from the iso-surface, which is why they must be projected back to the surface. To improve the sensitivity, shorter step sizes can be used but this will affect performance. Zhao suggests to adapt the step size to the local curvature. Streamlines are terminated when they approach other, previously found streamlines or when they leave the candidate area. A visualization of the curvature streamlines is shown in figure 3.6.

The last step is the clustering of the streamlines. The fact that the neck of a polyp is hyperbolic is used to select the candidate streamlines. Zhao first discards all streamlines that are not almost closed, and then selects from the remaining streamlines the ones that are hyperbolic. Next the winding angle is determined for the remaining streamlines. Using this technique only streamlines with a negative Gaussian curvature are selected. This is calculated by examining the individual principal curvature values, which should be negative in sign.

3.2. Flat lesion detection

In general, research towards the automatic detection of polyps has been fairly successful. Unfortunately this is not the case for flat lesion detection. Although there has been relatively sparse research,

it is already clear that the problem is very complex. The main reason is that, as opposed to polyps, flat lesions vary in shape much more [Soetniko et al. 2008]. Polyps are fairly well defined with a neck and a cap, but flat lesions are usually smaller, more sensitive to noise and do not necessarily have to protrude from the wall into the lumen.

No previous work could be found on the detection of flat lesions. Also, no research has been published yet about the question what features can be feasible for flat lesion detection. Because of this, we were forced to investigate potential features ourselves. We assembled a list of potential features in the previous chapter, and we will evaluate the feasibility of the mentioned features in chapter 7.

3.3. Colon wall visualization

Not much research has been performed towards the question whether it is possible to enhance the visualization of colon walls by improved rendering techniques. A lot of effort has been put in attempts to speed up the ray tracing algorithm in order to make it real time as well as in automated detection. Still, some improvements are worth mentioning.

3.3.1. *Unfolded cube*

Even though a colon gets inflated before the scanning process, the surface usually contains large folds that obscure a large part of the colon. Only when a viewer moves the camera over a fold, he is able to look between the folds by rotating the camera towards the formerly occluded areas. This required the reviewer to look all around him after each fold which obviously results in missed lesions. Serlie proposed to render not only the conventional projection plane in front of the camera, but all six faces of a cube placed in the scene with the camera as center point [Serlie 2001]. This cube could then be unfolded and projected onto a plane. This way, the reviewer can always essentially look in every direction at the same time without strong distortion of the shape of the colon, resulting in a considerable decrease of missed lesions (figure 3.7).

3.3.2. *Flattened colon wall*

Another attempt to solve the problems with the obstructing folds is proposed by Vilanova [Vilanova et al. 2001]. She flattens the colon wall and project it onto a flat surface (figure 3.9). This way it is possible to quickly review the whole of the colon including the areas between folds. Although not the first to propose the idea, she was the first to propose a method that is accurate enough in order to be considered for practical use.

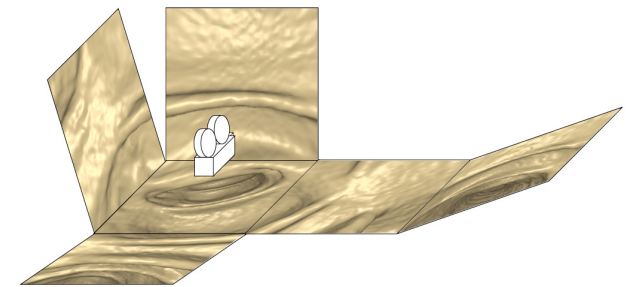


Figure 3.7 Unfolded cube

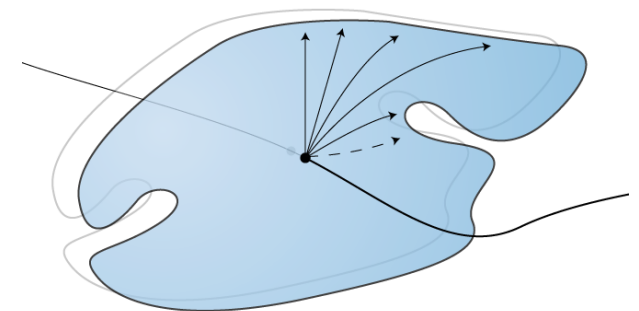


Fig 3.8 Nonlinear ray casting along the colon path 25

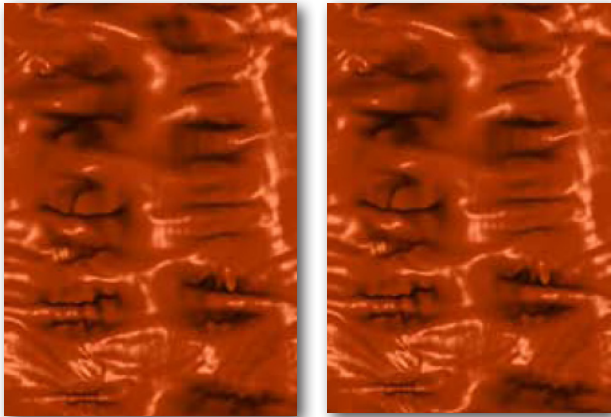


Figure 3.9 A flattened colon wall [Bartroli 2001]

First, the central path through the colon is extracted by thinning the mask of the lumen. The path is smoothed while ensuring that it does remain inside the colon. Next, a distance map is calculated. This distance map is a volume data set, where every voxel contains the distance from that point to the nearest point on the central path. This map is used to adjust the path of the rays in the next step.

The next step involves moving a coordinate frame along the path. For each position on the path, rays are cast in the plane orthogonal to the path, using constant angle sampling. This ray casting happens in a nonlinear manner, which means that the ray follows the negative gradient direction of the distance map calculated in the previous step. The result of this is that the ray is not straight but bends to the left if the central path is closer on the right side of the ray than on the left side and vice versa (figure 3.8). In effect, the ray moves as much as possible away from the path. Using direct volume rendering, the traced ray is terminated on the surface of the colon. The distance to the colon path is stored in a depth map.

This first step results in considerable distortions, which are partially removed using 2D scaling of the grid. This step adjusts the distances between the nodes in the depth map to their 3D volume counterparts using an iterative algorithm that moves the nodes in the right direction. Although an interesting approach, the amount of distortions is still fairly high. Also, there is a chance that polyps are missed near sharply curved areas of the colon path if the ray casting angle is not small enough. Hong et al. have extended the research towards shape preserving colon wall flattening [Hong et al. 2006]. However, some amount of distortion is inevitable, making this visualization technique only partially valuable.

3.3.3. Magic lens

Sometimes it can be useful to look behind the colon wall at certain places. Pickhardt published an evaluation of the magic lens technology (also called translucency tool) that shows the reviewer what HU values are inside suspicious areas (figure 3.10) [Pickhart 2004].

His main conclusions are that the translucency is quite useful for ruling out false positives like fat tissue or fecal residue. However, this tool does not adapt very well to the work flow of the radiologist; Usually radiologists use the orthogonal views to review a patient and use the 3D tool to get an idea about the shape of suspicious areas.

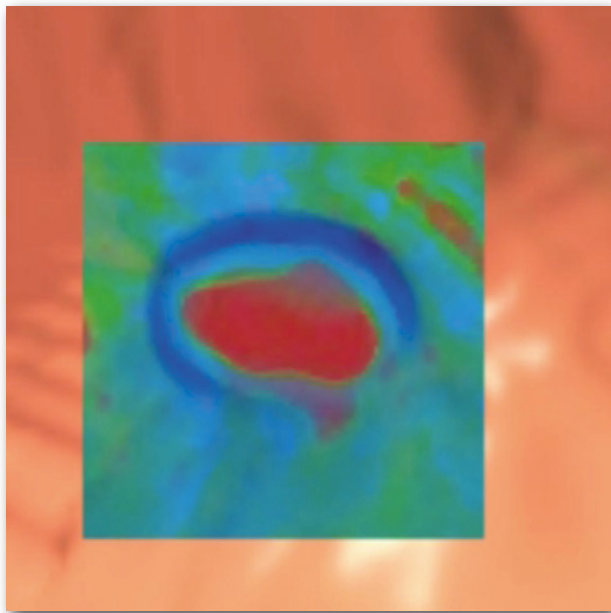


Figure 3.10 The translucency tool showing soft tissue.

3.4. Conclusion

Computer aided detection can not yet be applied as the only technique because there is still a chance the algorithm misses polyps. As a radiologist we spoke to put it: “CAD is the eye looking over your shoulder but not more than that”. Therefore, good visualization remains important.

Radiologists inspecting colons set two important requirements for the tools used to find lesions. First, the information they get presented by their tools needs to be accurate, and secondly, it has to enable them to perform their work as fast as possible. Therefore, although a helpful tool, we believe the flattened colon technique can be improved upon because they introduce distortion in the visualization. The unfolded cube is helpful but has the limitation that it has a fixed perspective angle. Besides that, the increased amount of information can also clutter the screen and increase the problem with the emphasis of the image. The magic lens is a tool and applying the technique to the whole colon wall would be impractical. However, if a radiologist has to select/deselect the tool every time he sees something suspicious, that would inevitably cost him a lot of time, thereby violating the second requirement.

In our research we will focus on techniques that will not cost the reviewer extra time and present the information to him as accurately as possible. We will define our research goals more precise in the next chapter.

4. Research goals and quality criteria

Now that we have some knowledge about the technical and clinical background and know what previous work has been performed, we try to frame our research goals in this chapter as a prologue to the following two chapters where we describe the techniques we tested. Not all techniques we examined turned out to be suitable for further research. Therefore, we add preliminary subjective evaluations in the next chapter, and we would like to describe the criteria used in this assessment in this chapter.

4.1. Research goals

Our research questions (see paragraph 1.2) state that we try to increase the number of found malignant lesions and/or to decrease the amount of time a review takes. Under radiologists, there is a strong prejudice against enhanced visualization techniques because it is possible that the visualization biases the judgement of the reviewer. We recognize this fear which is why we divide our research in two parts: enhanced lighting & rendering and feature based enhancements.

Proposed techniques will have to be implemented in Philips ViewForum, which excludes some techniques like global volume illumination in advance.

4.1.1. *Non-feature based enhancement*

The algorithms tested in this category will be described in chapter 6, and try to enhance the visualization by adapting or extending existing algorithms without integrating features of polyps and flat lesions in the algorithm. The techniques generally have a subtle effect and try to emphasize certain shapes while shifting other shapes to the background using variations of color, lighting and shadows.

Examples include the use of different lighting models or shadows. In figure 4.1 we see an example of a visualization with a single directional light. Although the shading help the viewer to define shape quite well, the specular highlights are of limited use. Because lighter areas usually draw the human eye more than darker areas, we would like improve the visualization by implementing lighting techniques that make important areas brighter while dimming other the areas. Transparency can be seen as a non-feature based enhancement as well, although we did try to adapt it to some features. Those variants will be discussed in the next chapter.

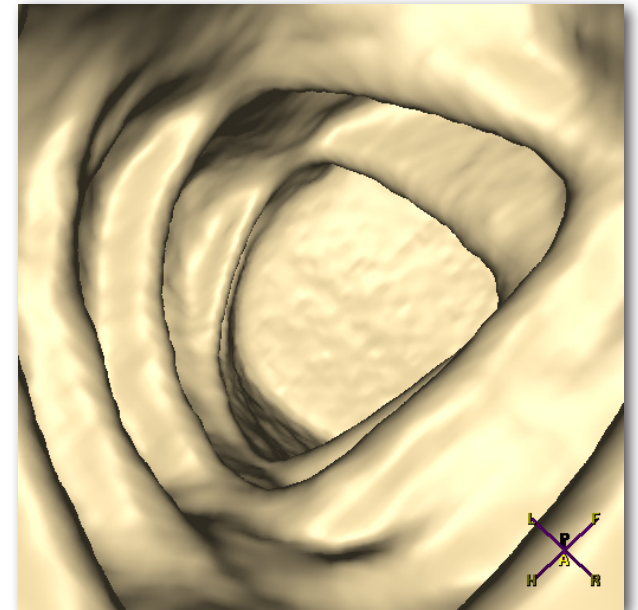


Figure 4.1 Example of a visualization with a bad emphasis. Note how the specular light draws the eye to uninteresting areas

4.1.2. Feature based enhancement

Feature based enhancements try to visualize features in order to give the reviewer a better understanding of the colon. As stated, the main problem with features is that the relationship between features and lesions is not one-to-one. It can be that a certain area has all the features of a flat lesion, but does not show a flat lesion at all. This way, the visualization introduces a bias in the interpretation.

That said, the visualization as applied in the Philips ViewForum software does not convey any more information than the surface curvature. It does not even get the curvature completely right; everything below a fluid surface is not visualized and faeces can seriously deform the visualized wall. Moreover, all sorts of information are left out. Examples include wall reflectivity caused by wetness and wall color, and what can be seen behind the wall like nearby organs.

The question that remains is which information is considered by a radiologist to assist him in his work, which means it either helps to find more colon lesions or shortens the time a colon review takes. This inherently means he will not be interested in the location of the organs or his orientation in the colon, to name a few examples, but instead that he possibly is interested in which areas are contrast fluid and which are not, because adhering contrast might be a feature of a flat lesion.

With these side conditions in mind we tried several techniques that could enhance the radiologists' understanding of the colon. Examples include the raised grey level values of flat lesions, contrast fluid that might indicate a flat lesion, and curvature information. These techniques are discussed in chapter 7.

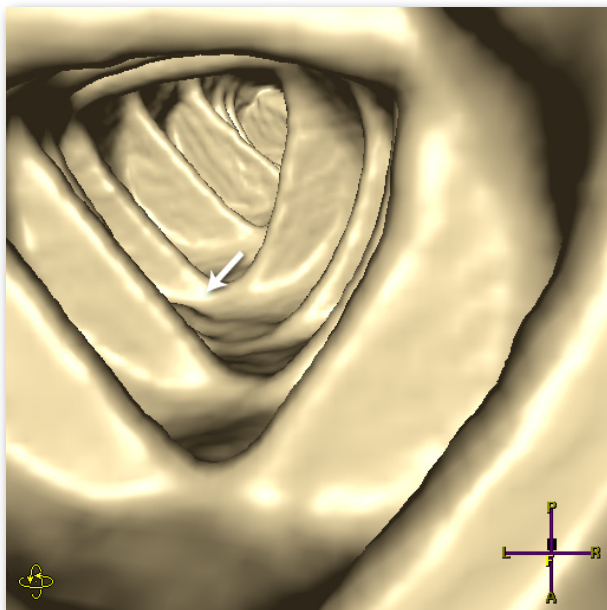


Figure 4.2 The Philips Viewforum ray tracer

4.2. Quality criteria

As a benchmark we use the Philips ViewForum ray caster. This ray caster is a high performance iso-surface renderer that is not extended with additional visualization techniques. For shading, Phong shading is applied as discussed in chapter 2. A dark yellow color is used for ambient lighting, and a slightly yellow directional light with high intensity is used as the main light. This directional light is placed at the location of the camera. All techniques will be evaluated relative to this ray caster.

We evaluated every technique using test data from the Amsterdam Medical Center. This test data consisted of prone/supine patient data with typically around 450 slices (Appendix A). To ensure consistency in this thesis we rendered all images relative to figure 4.2 which shows a typical location in a colon. The elevation in the middle of the image between the folds is a flat lesion that is covered with

a thin film of contrast fluid. This particular flat lesion will not be missed by a reviewer but a flat lesion like this could easily have been missed when it would have been located at a less easy to spot location.

As benchmark criteria we use the following criteria:

4.2.1. Object size

The object size defined how well the technique in question is able to visualize different sized objects. Small objects are objects sized less than a millimeter and usually consist of noise, which is why we usually do not want to visualize these objects. Mid-sized objects are objects from a few mm up to 20 mm. This is the category where most polyps and flat lesions are located. Large objects are shapes larger than 20 mm. Examples are folds and large tumors (figure 4.3).

4.2.2. Usability

The usability of the techniques can be measured with two criteria. First, the consistency describes how similar objects look from different angles and distances. This is important because this helps a reviewer to associate shapes that represent the same object. Secondly, the intuitivity determines how quickly a reviewer understands what he sees without additional knowledge (figure 4.4). In figure 4.4, not all the red areas represent blood. For example, the flat surface at the bottom represents contrast fluid. The fact that it is colored red is a typical lack of intuitivity. A technique might successfully display additional information about the visualized colon wall, but still fail to improve the review time.

4.2.3. Technical criteria

Some techniques are very sensitive to noise which inherently makes them perform worse near flat lesions, which is why we include a noise sensitivity criterion. The computational speed judges the speed of the algorithm.

4.2.4. Flat lesions and polyps

The last criteria judge how well the technique is able to visualize flat lesions and polyps. Of course these will be a result of other criteria and determine our final opinion of the technique.

After each paragraph, we will include a table structured as follows:

| | small objects | mid-sized objects | large objects | consistent | intuitive | noise sensitive | flat lesions |
|-------------|---------------|-------------------|---------------|------------|-----------|-----------------|--------------|
| Viewforum | 0 | 0 | 0 | 0 | 0 | 0 | 0 |
| Technique 1 | + | - | ++ | 0 | 0 | + | 0 |
| Technique 2 | 0 | ++ | 0 | .. | | | |

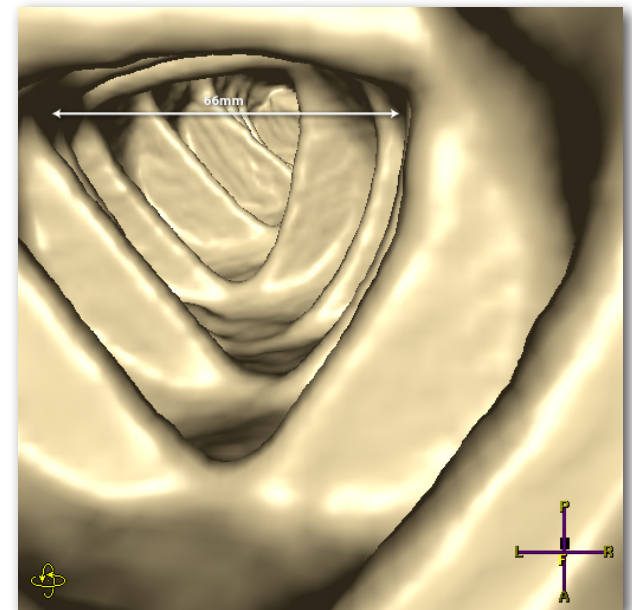


Figure 4.3 Typical diameter of a colon. The flat lesion is 6 mm. The white line is 26 mm in length

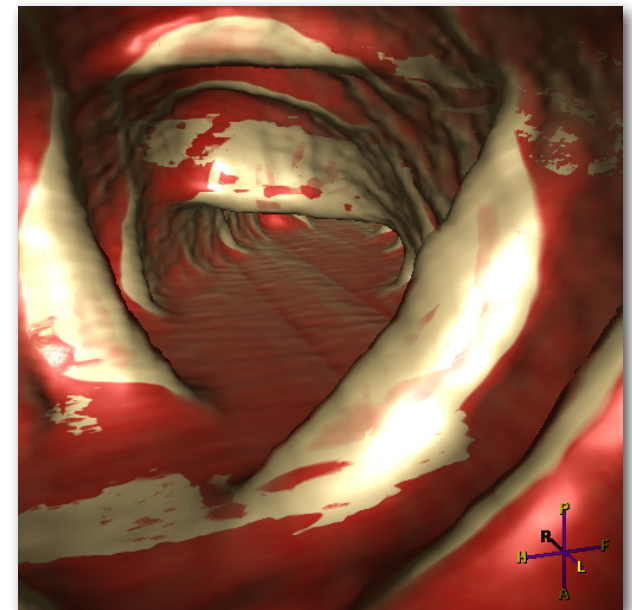


Figure 4.4 Example of an unintuitive technique. Note how the algorithm tries to show blood, but colors fecal residue red as well. Using realistic colors usually is risky.

Every criterion is measured on a scale using one or two pluses or minuses which are ranked relative to the Philips Viewforum renderer. Zero represents a result comparable to the Philips visualization, whereas one - or one + represents a medium change. One - does not have to be a problem, and a + does not have to be a solution. - - and ++ represent considerable changes and represent respectively major problems and great outcomes. Judgements are made by the author only, which inevitably introduces a prejudice. Therefore, we also evaluate the most promising techniques with an expert evaluation. We will only include those criteria that we deem most important or striking.

Now that our research goals and evaluation criteria have been defined, we can continue with the techniques we have tested. In the next chapter we will start with the lighting, shadows and shading techniques, after which we will take a look at feature-based techniques.

5. Enhanced rendering: lighting, shadows and shading

We first attempt to find enhancements by extending the default visualizations by adjusting rendering parameters like lighting and shading models. This approach aims to be as general as possible in order to avoid the risk of suggesting things that are not there.

We first looked at different lighting models, and several related techniques. After that, we considered using some form of shadowing. Lastly, we tried adjusting the shader directly in order to show information from behind the surface.

The best results in this and the next chapter will be evaluated in more detail and with more data sets in chapter 8. In this chapter we will only include a subjective assessment of the techniques that will show how the techniques behave compared to each other.

5.1. Lighting models

Lighting is known to play a major role in the visibility and also the appeal of an image. Several models were evaluated. Some standard models like point and directional lights were tried, as well as some more advanced models such as the tube-light, the three-point lighting and the rim lighting. Some alternative models were left out for reasons discussed in 5.1.6

5.1.1. *Point light*

The point light is the basic light model and is comparable with a light bulb. A uniform amount of light is emitted in all directions. The light is placed at the location of the camera, from which it follows that the light rays coincide with the camera rays (figure 5.1).

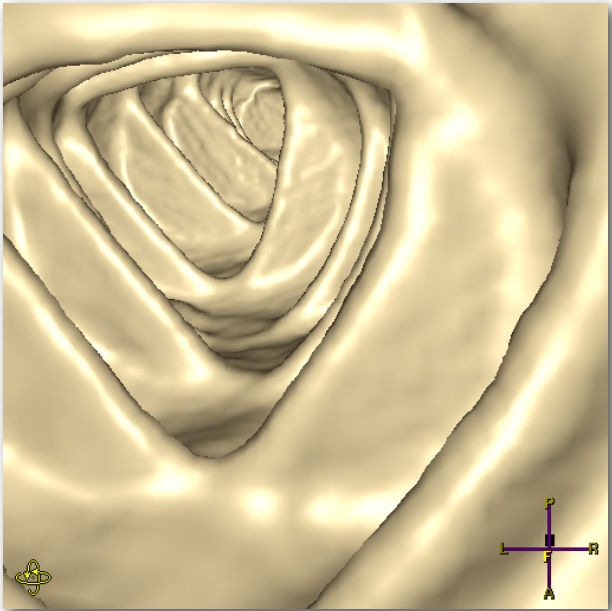


Figure 5.2 Point lighting

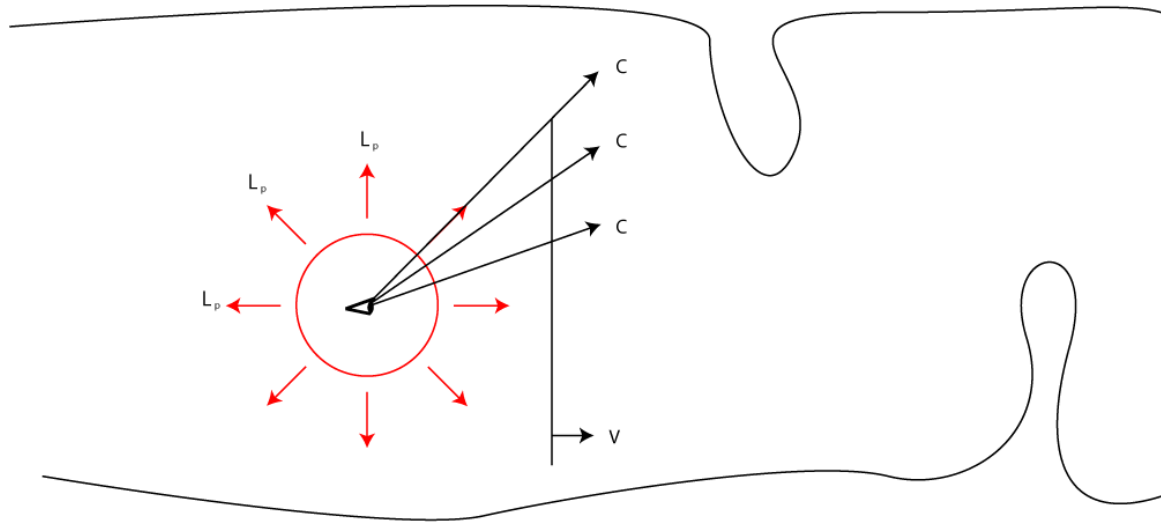


Figure 5.1. Point lighting. Note how the camera rays C coincide with the light rays L_p , but not with the view plane normal V

Because the light rays are exactly parallel to the camera rays, the result is a very evenly lit picture (figure 5.2). In turn, the consequence of this is that small details are hard to spot, and that the reviewer's eye is not drawn to specific parts of an image, which we feel can be improved upon. An advantage is that variations on the surface and orientation of the surface are all visualized exactly in the same way independent of camera rotation, but a severe downside is that the slightest variations are only visible as very small variations in brightness, making them very hard to distinguish. Moreover, specular highlights in the image appear only where the surface is parallel to the view plane. This mirroring reflection happens because the viewing direction is almost the same as the reflection vector, which is in this case orthogonal to the rendered surface.

5.1.2. Directional light

A directional light is used in the Philips ViewForum software and can best be compared with light emitted from the sun. The effect of the light depends on the rotation of the light and not on its location. In the Philips ViewForum software, a single directional light is rotated so that the light direction coincides with the view plane normal (figure 5.3). Note how this differs from the point light where the light rays coincide with the camera rays when the point light is located at the location of the camera.

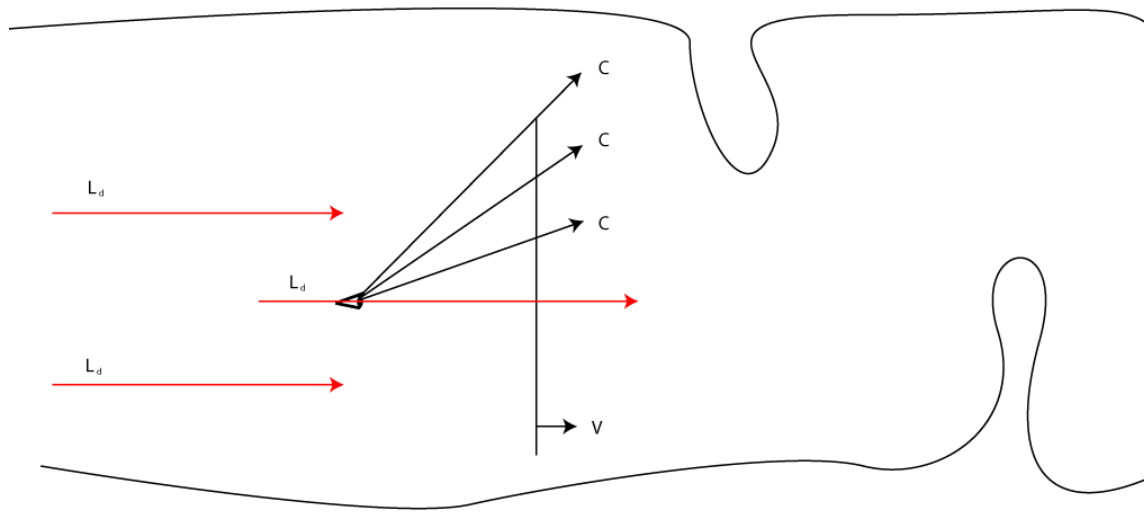


Figure 5.3 Directional light. Note how the light rays L_d coincide with the view plane normal V

We expected the directional lighting to perform worse than the point light because the colon is usually oriented parallel with the view plane normal and thus the direction of the light. This would darken the sides of the colon wall and emphasize the faces of the folds that are oriented perpendicular to the view plane normal. Moreover, rotating a camera changes the color of an object, something we expected to appear unnatural. For example, small bumps in the wall will stand out when the view plane normal is parallel to the colon wall and will be almost invisible when looked at directly.

However, the directional light did not perform bad at all (figure 5.4). Indeed details on the wall were overemphasized when that part of the wall was orthogonal to the view plane normal and underemphasized when parallel but this did not appear unnatural. On the other hand, another downside of the directional light is that the specular component (the shininess) only causes the light to reflect on places where the wall is parallel to the view plane (which is because the rotation of the light is more or less the same as the rotation of the eye vector). Although the specularity does help the viewer to perceive shape, it also appears in quite a random manner. It is helpful in a number of places but it seriously occludes details in other locations.

Nevertheless, directional light performs better than point lighting. There are more differences in intensity in the images which helps the reviewer to distinguish shape. The change of color depending on camera location appears not to be confusing but helps the reviewer perceive shape.

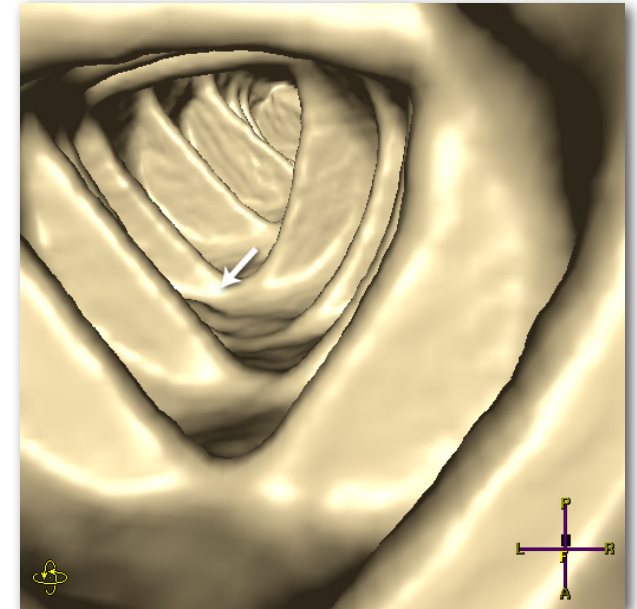


Figure 5.4 Directional lighting

We also did some tests with directional lights with different orientations. However, as also discussed in 5.1.6, the problem with this is that this rotation would either have to depend on the colon wall or would introduce an unwanted bias. 5.1.5 discusses rim lighting which is comparable to a directional light that is rotated 180 degrees.

5.1.3. Tube lighting

The tube light is inspired by overhead office lighting. Obviously, no polyps are found in an office environment but the office lighting is known to provide a very evenly lit environment that is very suitable for every-day work. By putting a curved linear light at the center of the colon lumen, we expected the more even lighting would help objects stand out better (figure 5.5). For every point on the surface, the closest point on the light curve is calculated. This point is then treated as a point light.

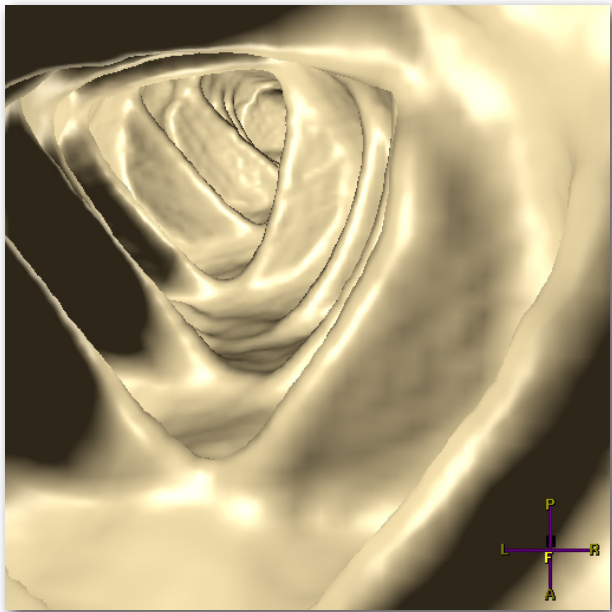


Figure 5.6 Tube lighting

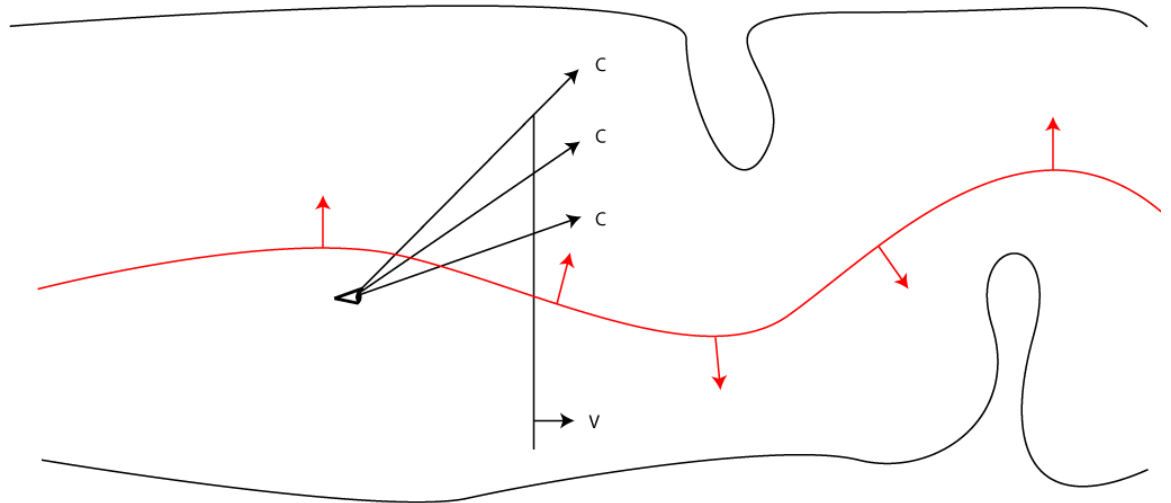


Figure 5.5 Tube lighting. The light rays are not dependent on the camera

This lighting model proved to be a failure, and we abandoned the tests after the first results. The main problems are twofold. Firstly, the difference in lighting is dependent on how the wall is oriented towards the centerline (figure 5.6). A wall facing the curve is lit very evenly, while tissue at the side of folds appears very dark. The second downside is similar to what we feared with the point light: small details became almost invisible because of the evenly lit surface. Variants of this type of lighting will suffer from the same problem which is why we lost faith in this lighting model.

As a side note we can mention that the reason office lighting works so well is that it is much brighter than most other lights. Also, indeed office lighting lights an area quite evenly but light bounces off

objects a lot which, in combination with the high intensity, ensures all objects are lit well. The lack of this latter feature renders the tube lighting model useless. We will look into a variation of global illumination in the next paragraph. Moreover, in offices an evenly lit environment helps people to read books and use their screens better. In colon lumens, it is the unevenly lit nature of the light that helps distinguish shapes.

5.1.4. Three-point lighting

Three-point lighting is a technique inherited from the cinematographic world and is especially designed to help objects stand out from their background.

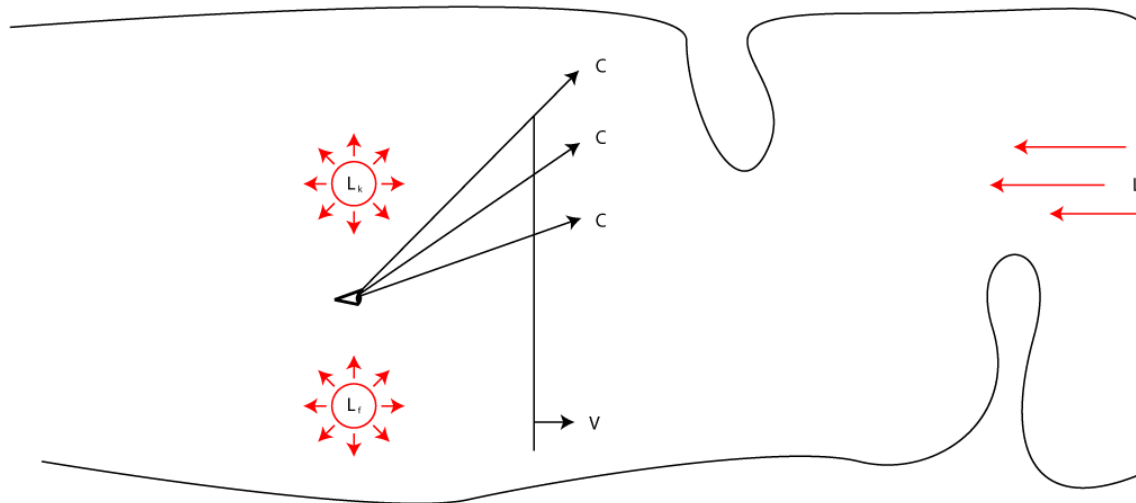


Figure 5.7 Three-point lighting: Key light (L_k), Fill light (L_f) and the Rim light (L_r)

The lighting composition consists of three lights (figure 5.7). The main light is called the key light and is the main source of illumination. Usually this light is to the left or right of the camera to create asymmetric lighting conditions for esthetical reasons. The second light is called the fill light, and fills any harsh shadows cast by the primary light. This light is usually positioned opposite to the camera from the key light. The last light creates the effect we were after and is called the rim light. This light is placed behind the object and faces the camera but is placed out of sight (so either slightly left or right from the image or behind the object - in a virtual application it is easy to just hide the light itself). This way it creates a rim of light around the objects, helping viewers to distinguish it from the background. All lights are fixed in position relative to the camera location (figure 5.8). The distance of the primary and fill light to the camera are equal. This distance is dependent on the object size, we put them at a distance of a quarter of the colon wall away from the camera. We attempted to ensure that the total

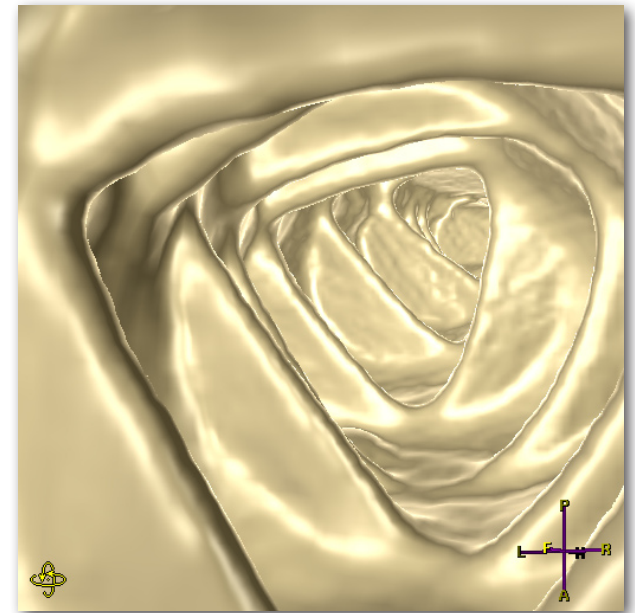


Figure 5.8 Three-point lighting

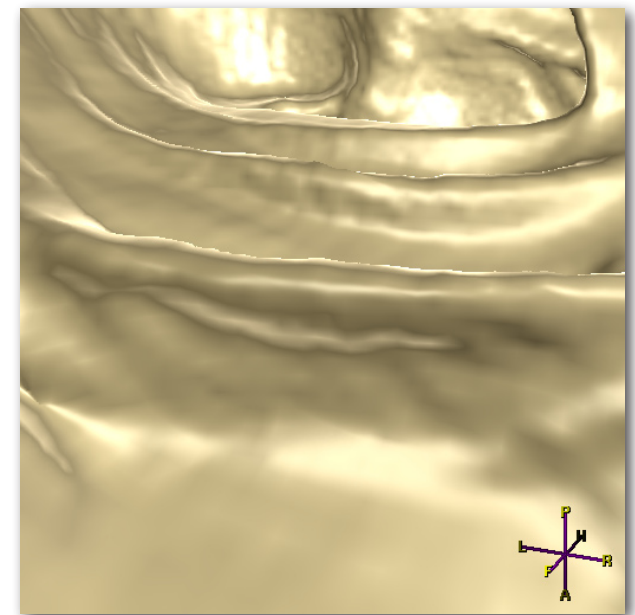


Figure 5.9 Unpredictable nature of three-point lighting

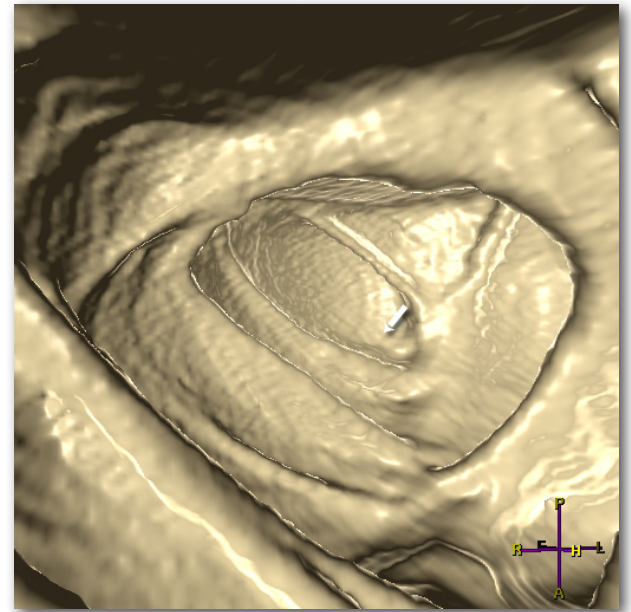
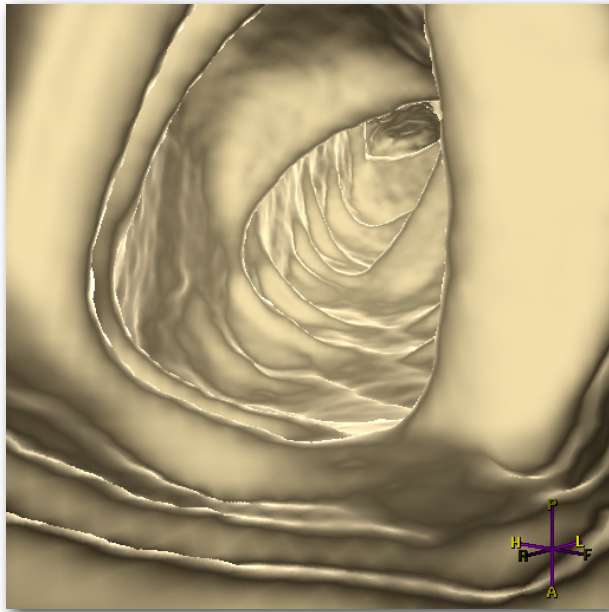
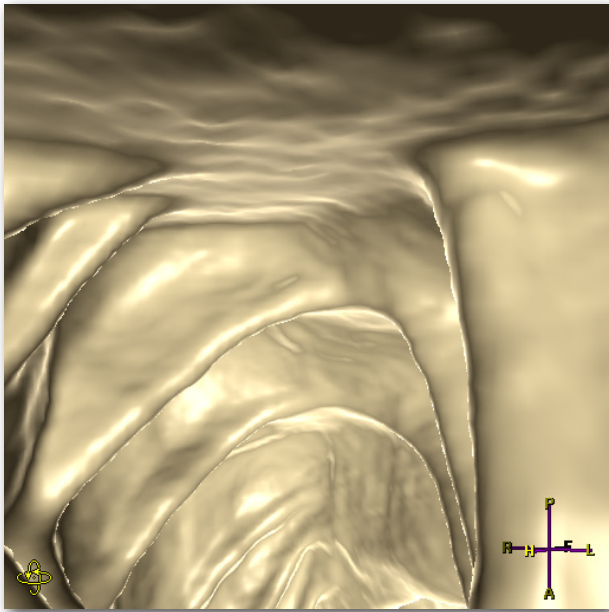
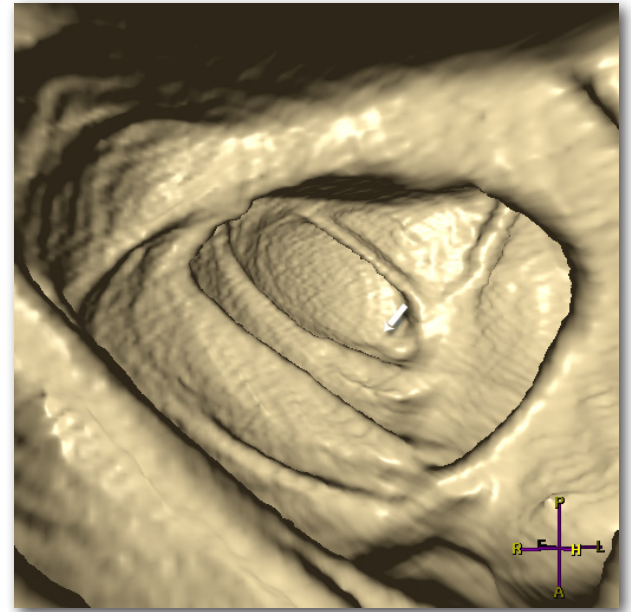
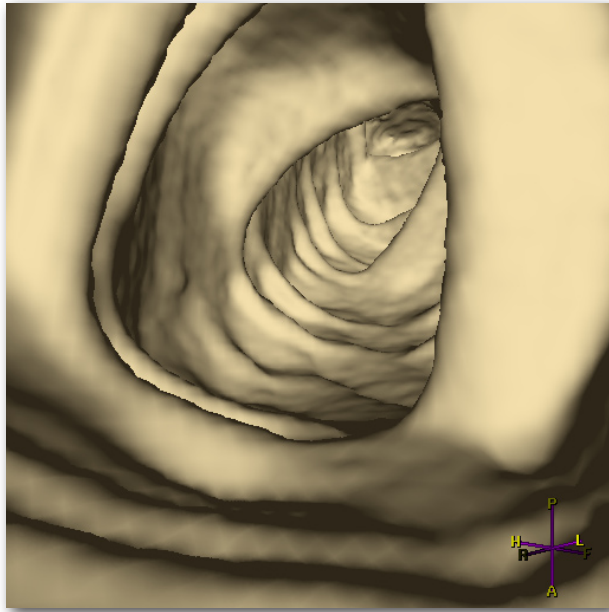
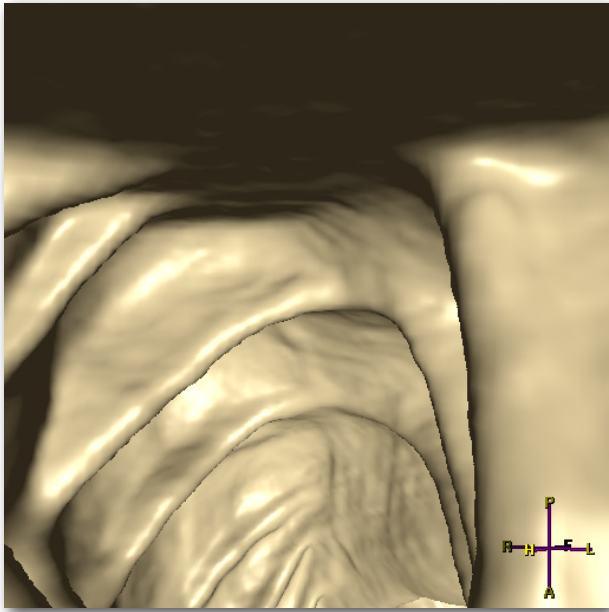


Figure 5.15 Rim light has the tendency to overly light walls when closing in on them

Figure 5.16 Small details are visible on the walls

Figure 5.17 The rim light fails to accurately emphasize very flat lesions

intensity of the two lights equals the light emitted by the single light in the point and directional lighting images.

Three-point lighting proved to be too sensible to camera movement. Because the main lights are placed slightly away from the camera, rotating the camera when near a wall results in unexpected artifacts. For example, the lights can render small spots on the wall when the lights are near the wall. Of course, the aesthetic aspect is of secondary importance to us so replacing the key and fill lights with a single point light solves this problem. Still, moving the camera also moves the backlight which makes the renders very sensitive to slight camera movements.

A second problem is that the directional back light generates too little rim. We tried to overcome this problem by replacing it with a point light. However, this creates unexpected lighting conditions on the location of the point light, which cannot be but too far near the back.

Three-point lighting was not much of a success but it opened the door for a derived technique, pure rim lighting. For a discussion on related techniques we refer to 5.1.6.

5.1.5. Rim lighting

Rim lighting is not a technique using conventional lights but could best be described as an extension to the Phong lighting equation. Because it is so closely related to the three-point lighting, we discuss it here.

Although the three-point lighting has some considerable downsides, it successfully shifts the focus of the visualization from lighter (uninteresting) parts to the rims. By modifying the algorithm we tried to exploit this fact.

The rim light I is calculated during the evaluation of the color of the wall. After the color of the surface has been calculated, the rim light is calculated using the eye vector and the normal vector of the surface as follows:

$$r = 1.0 - \|\vec{I} \cdot \vec{N}\|$$

where I denotes the vector pointing from the point on the surface to the camera and N the normal vector at the location of the surface. This term r results in a factor with a range between 0.0 and 1.0 and is multiplied by the texture color of the wall after which it is added to the Phong equation. This approach can also be illustrated using figure 5.11:

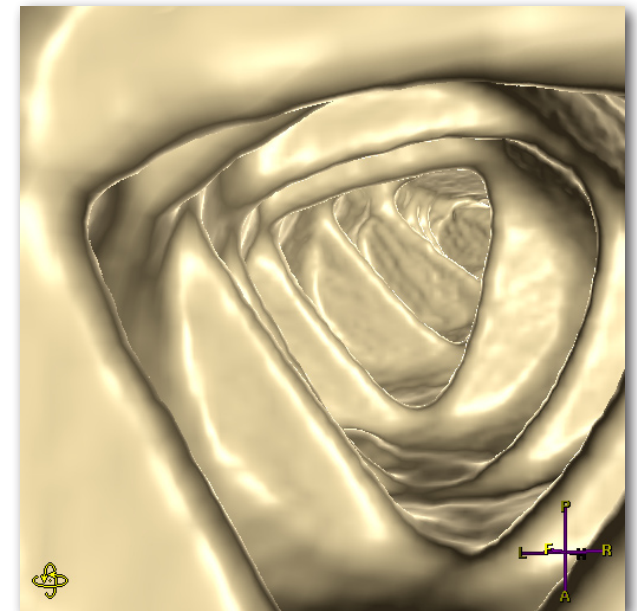


Figure 5.10 Rim lighting

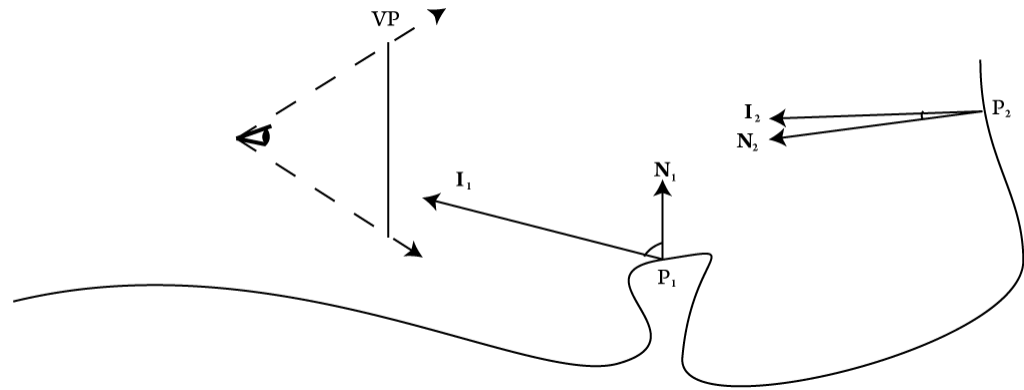


Figure 5.11 Rim lighting

N is the surface normal and I the vector pointing to the camera. The dot product of N_1 and I_1 at point P_1 will be much smaller than the dot product between N_2 and I_2 at point P_2 . The smaller this dot product, the stronger the rim light term will be. If the resulting rim light term is small enough, we multiply the color of the texture with the rim light term and a constant, which keeps the resulting color within the color range of the image, which in turn makes it easy and less disturbing on the eye.

This worked reasonably well, however, as can be seen in figure 5.12, the amount of rim light differs based on the location of the rendered pixel on the view plane. This can be explained with figure 5.13 where we see an exaggerated sketch of the problem.

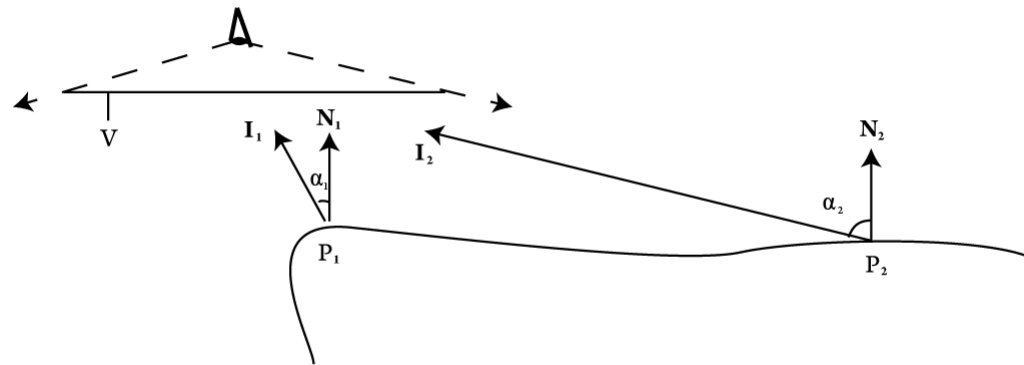


Figure 5.13 Rim lighting near an edge

As can be seen, the dot product not only depends on the normal vector N and the orientation of the camera but also on the angle of the ray I that is cast through the view plane in comparison with the view plane normal V . In other words, a small alpha results in a larger dot product between I and N which in turn results in a smaller rim light term. We would expect the rim light at point P_1 to be the same as at P_2 . However, the fact that point P_2 is located such that the eye vector differs more from the view plane normal results in a stronger rim light factor at point P_2 . This effect will be stronger when the viewing angle of the camera is larger. A first thought might be to use the normal vector of the view plane instead of the camera vector as in the following formula:

$$r' = 1.0 - \|\vec{V} \cdot \vec{N}\|$$

where V is the (inverted) view plane normal vector. The problem with this approach can be seen in figure 5.14. Because the view plane normal is generally oriented in the direction of the center line and thus roughly parallel to the colon wall, the normal vectors of the wall are orthogonal to the view plane normal, resulting in very strong rim light effects. This will be a problem when the camera is oriented more or less parallel to the wall which happens regularly.

Another solution is to compensate for the location on the view plane by multiplying the rim light with a factor as follows

$$r'' = r + 1.0 - \|\vec{I} \cdot \vec{V}\|$$

The first term is our original rim light. As we saw before, the strength of the bias is dependent on the angle between the view plane normal V and the eye vector I . In other words, the larger the dot product between the view plane normal and the eye vector, the more bias is introduced. The last term tries to remove this bias by subtracting this dot product. This removes the bias introduced by the difference between the view plane normal and the eye vector (figure 5.10).

The rim light successfully emphasizes other areas of the visualization. However, the new emphasis is still not the emphasis we want. As can be seen in figure 5.15, the rim light can be fairly sensitive to noise and draws the eye towards this noise. This is caused by the fact that the rim light overly emphasizes rims, and thus small variations like noise are exaggerated as well. Also, rim light tends to overly light flat areas like fluid levels when the camera view plane is oriented perpendicular to a flat areas. On the other hand the rim light successfully emphasizes small details that would otherwise have been hidden in shadows (figure 5.16). Lastly, we included a visualization of a situation where the rim light fails to accurately emphasize a flat lesion (figure 5.17).

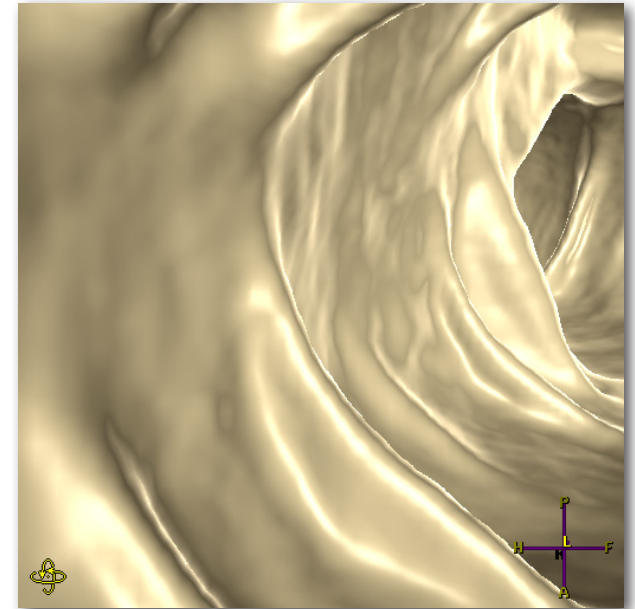


Figure 5.12 The effect of rim lighting depends on the location on the view plane which can be noticed in the upper right part

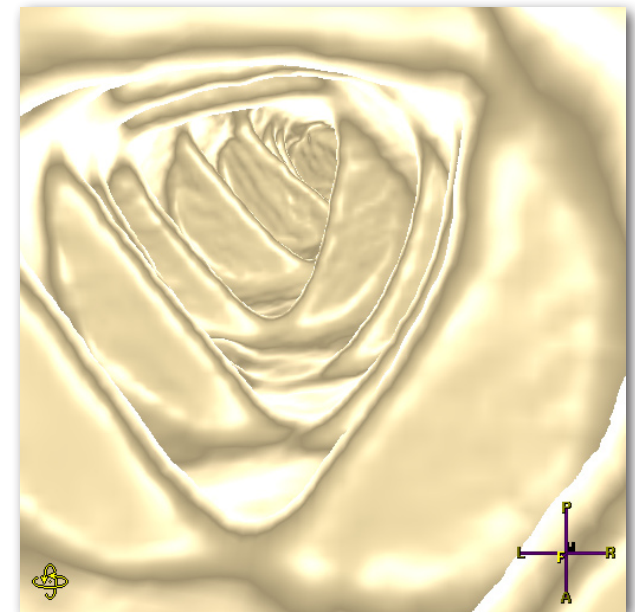


Figure 5.14 The view plane normal is orthogonal when the view plane normal is parallel to the colon wall

5.1.6. *Other lighting techniques*

Several other possible modifications to the standard lighting model are possible. We have not tested these modifications and we would like to defend these choices because we believe there are fundamental problems with them which prevents them from contributing in a positive way to the amount of found lesions or the speed with which they are found. We only discuss techniques that could have been applied in the ViewForum renderer, which is one of our boundary conditions.

Multiple light sources

It might be possible to place multiple light sources independent of the camera in the colon. One could evenly place point lights on the central path and introduce an intensity falloff to ensure the lights only affect their direct vicinity. However, we think these techniques inherently introduce either a bias or contain a random component. For example, when one places lights along the path, it would be hard to choose the optimal amount of spacing between lights because one would have to depend either on features of the colon wall or on a random factor. The former inevitably introduces a bias, and randomness is what we want to avoid because that causes us to be less able to predict what the user will see. Moreover, structures on the colon wall that have the same shape would appear different dependent on the orientation of nearby lights.

Camera dependent light sources

It might also be possible to make the lighting dependent on camera location and orientation. However, again we would have to use features of the colon or introduce a random factor. Like with the multiple light sources, using features of the colon would introduce a bias because we would have to interpret the colon wall and introduce certain assumptions about polyps and the colon wall. The problem is that these assumptions are based on polyps that are not causing problems; the polyps which are hard to define are the ones that cause problems. We already see the problem that a random factor causes prominently with the three-point lighting where the primary and fill lights cause unwanted artifacts.

Interactive lighting

Another idea might be to enable the reviewer to adjust the lighting whenever he sees fit. Although this potentially could give the reviewer a better idea of what he is looking at, this would violate one of our boundary conditions defined in chapter 4.1 where we assumed that a radiologist inspects a lot of colon walls and that the use of additional tools would slow him down considerably. In order to be viable for a radiologist, the tool would have to add considerable value, which we believe a different lighting cannot offer.

A tool also interferes with his standard workflow; A radiologist usually inspects the orthogonal views as a primary method and refers to the 3D visualizations near suspicious areas. This way, the 3D visualization already acts as a tool.

5.1.7. Subjective assessment

We assess the quality of the presented techniques as follows:

| | small objects | mid-sized objects | computational intensive | consistent | intuitive | noise independent | found flat lesion rate |
|----------------------|---------------|-------------------|-------------------------|------------|-----------|-------------------|------------------------|
| Viewforum | 0 | 0 | 0 | 0 | 0 | 0 | 0 |
| Point lighting | 0 | 0 | 0 | + | 0 | + | 0 |
| Directional lighting | 0 | 0 | 0 | 0 | 0 | 0 | 0 |
| Tube lighting | - | - | - | + | -- | + | -- |
| Three-point lighting | 0 | 0 | 0 | -- | - | 0 | - |
| Rim lighting | + | + | 0 | - | 0 | - | + |

Point lighting is rated slightly more consistent than directional lighting because the resulting wall color does not depend on the orientation of the camera. However, point lighting, while being slightly more consistent and noise independent, is not likely to increase the number of found polyps during a review. This is mainly due to the fact that the irregularities generated by a directional light help the reviewer see objects under different circumstances. Tube lighting proved not to be very intuitive and unable to light any size objects better than directional lighting. Three-point lighting proved to be very inconsistent due to the fact that three lights positioned at fixed distances from the camera moved with the camera. Rim lighting overly emphasized small objects and noise, generating slightly cluttered images. Also, depending on the camera rotation relative to an object, an object might look considerably different. However, we found that the algorithm was able to emphasize part of the flat lesions and polyps, which is why we evaluate this algorithm with experts in chapter 7.

5.2. Shadow models

Shadows are essential in the real world to help people perceive shape. Mishra showed that the use of shadows in endoscopic applications can increase the performance of reviewers [Mishra et al. 2004]. Therefore, it seems a reasonable thought to add shadows to the visualization in order to enhance them. We applied two kinds of shadowing techniques to the colon visualization. The first is the conventional

standard shadow technique present in every ray tracer. The second, called ambient occlusion, tries to mimic real life shadows more realistically.

There are more shadow models possible than discussed here, however, as stated in chapter 4 we have to limit ourselves to the iso-surface renderer in the ViewForum software.

5.2.1. Shadows

Strictly spoken, a point on a surface is in shadow when it is blocked from the light and no light is reflected at that point. Note that this differs in definition from occasions where the dot product between the light ray and the normal vector is negative or close to zero; although the light does not have any effect, we do not define this as an object being in shadow. This is important, because without any shadows a rendered image still has lighter and darker areas caused by the shading. However these areas are defined by the location and orientation of the light and not by the fact that objects are blocking light. The math is straightforward: for every surface that is rendered we check for every light whether the path to the light is blocked by something. Based on this criterion we either do or do not apply the diffusion algorithm for the given light. If a point is in shadow we only apply the ambient light.

In our test visualizations we only applied shadows in its most basic form, which means we did not test other light source sizes than zero and no multiple light sources. When using one light, placing the light at the location of the camera will not generate shadows for trivial reasons. Therefore, in figure 5.18, we placed the light somewhat further down the colon on the central axisto show the effect.

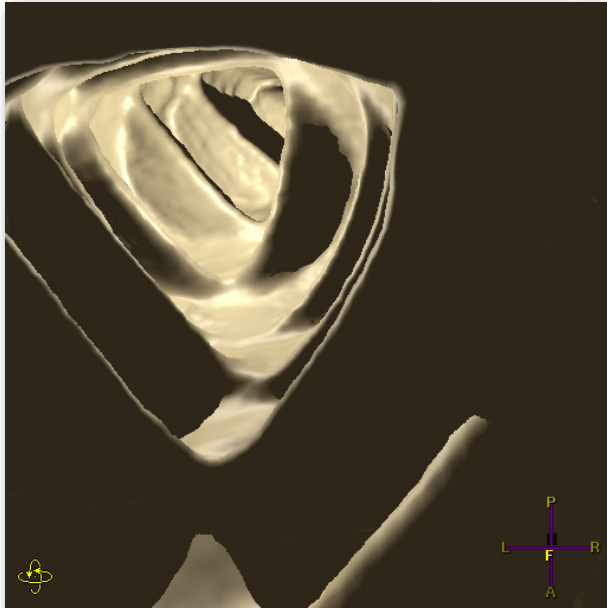


Figure 5.18 Strict shadows. For clarity,, the light was placed a little further down the colon path

As can be seen from figure 5.18, shadows generated by a single local light source do not give us a very realistic image because of the lack of diffuse reflection at locations in shadow. This is because in a real world situation light is bounced via other surfaces, generating smooth gradients in the shadow and almost never areas that are completely dark. Shadows as in the image do not help us distinguish shapes. The color of areas that are in shadow is only determined by the color of the ambient light, thereby removing any definition of shape.

Another problem with this type of shadows is the sharp shadow lines. This can be avoided by assigning a size to the light and by calculating for every point how much of the light is visible. This usually results in considerable computational overhead, and these gradients can interfere with the diffuse reflection algorithm, thereby distorting the reviewers perception of shape. It would be possible to place multiple lights in the colon to generate a more realistic interplay of light and shadow. However, we do not think this will lead to a solution for the same reasons as discussed in 5.1.6.

5.2.2. Ambient occlusion

The main reason that shadows as discussed above are of limited use is that it does not incorporate light bounced off objects nor the physical size of the light source. Global illumination techniques try to overcome the former problem by not only taking light directly from the light source into account but also indirect light from the same light source bounced via objects and surfaces. There are numerous algorithms that attempt this of which radiosity and photon mapping techniques are probably the best known [Jarosz et al. 2008]. However, they all share a common downside, which is computing time. Most global illumination techniques require many minutes to hours to render at an adequate quality and are thus in their unaltered form useless in a real time volume ray tracer. Optimizations can be achieved by porting the algorithm to the GPU or by performing part of the algorithm in advance.

One particular form is of more interest to us, namely the ambient occlusion technique. This technique tries to calculate a ratio of occlusion for a particular point \mathcal{P} on a surface by examining the hemisphere at the side of the surface normal. This ratio serves as a measure for the amount of light reaching the surface at that point. The main advantage is that ambient occlusion is a light-independent technique which allows it to be pre-calculated.

The ambient occlusion algorithm can be mathematically described as:

$$A_p = \frac{1}{\pi} \int_{\Omega} V_{p,\omega}(N \cdot \omega) d\omega$$

Where A_p is the calculated occlusion at surface point \mathcal{P} , V is the visibility function for the hemisphere ω at point \mathcal{P} and N is the normal vector at \mathcal{P} :

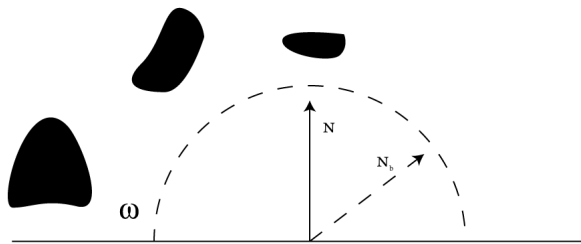


Figure 5.19 Ambient occlusion

The visibility function is usually approximated using a Monte Carlo implementation. For every surface corresponding to a pixel in the rendered image, a number of vectors is randomly generated using a random generator that generates vectors with a uniform distribution on a half dome defined by the normal vector of the surface (figure 5.19). These vectors are traced from the surface into the object

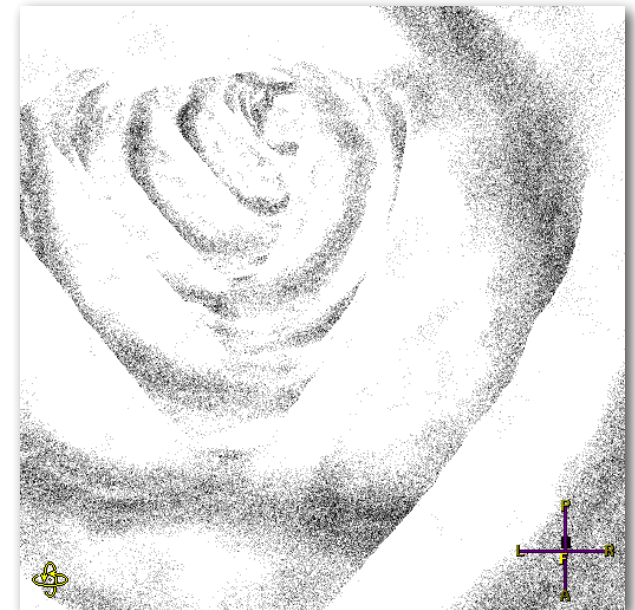


Figure 5.20 The ambient occlusion factor in every pixel. We used 4 rays per pixel and a maximum depth of 10 voxels.

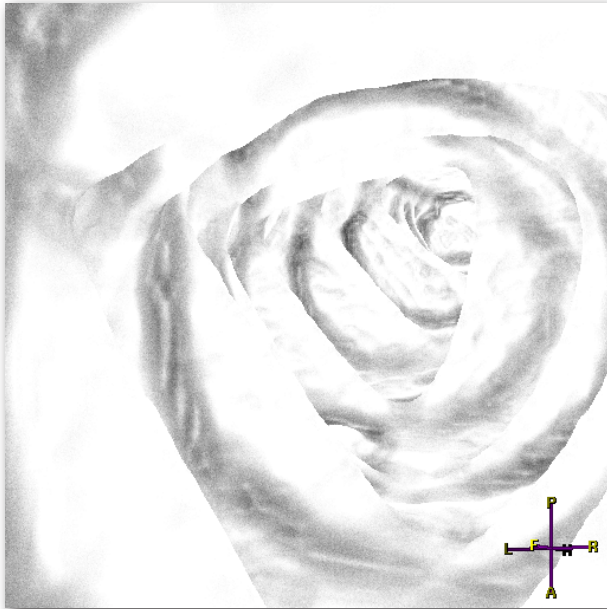


Figure 5.23 Ambient occlusion, 128 rays per pixel cast 3 voxels deep

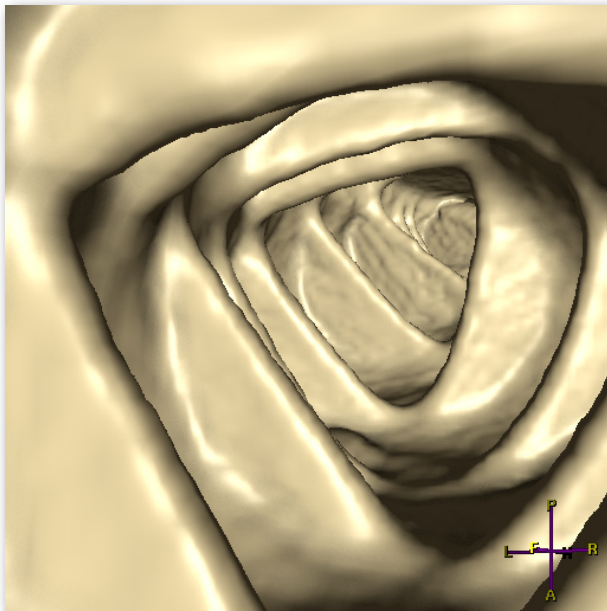


Figure 5.24 Ambient occlusion. Notice how the result is not distinguishable from the normal render

space, and for every ray is checked whether the ray hits an object. Dividing the amount of rays that hit an object by the total amount of rays results in A_p which lies in the 0.0 - 1.0 range. This ratio defines how occluded the surface is. Figure 5.20 illustrates the result of an ambient occlusion pass where 4 rays are cast per pixel. This number is chosen to give the reader an idea of the random behaviour of ambient occlusion. The maximum depth of a ray was chosen to be 10 voxels which makes the algorithm not sensitive to the folds but mainly to smaller structures.

When applied to colon walls, the ambient occlusion algorithm does not work too well. First, we need to compensate for the fact that the colon wall is a closed surface. Rays cast from the surface of the colon wall will always hit another surface. Therefore, we need to define a maximum distance, after which we can conclude the ray hit nothing. We initially tried to set this distance at half the colon lumen which is approximately 30mm. The colon differs in diameter based on the location in the colon which is why this choice is somewhat arbitrary.

The second problem is that the algorithm works very well in tight and sharp corners. In these areas a lot of rays will hit the nearby surface resulting in a high occlusion ratio. Colon walls usually have a smooth surface and are therefore less sensitive to the algorithm. To compensate for this, we tried to limit the dome in which the rays are cast (figure 5.21)

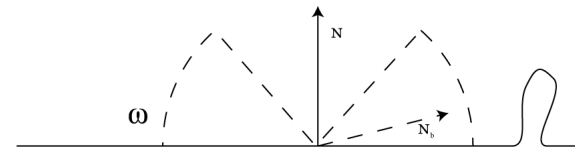


Figure 5.21 Applying a limited dome in ambient occlusion

This resulted in the algorithm being too sensitive. Because the surface is not as flat as in the illustration, lot of the rays were now cast directly into the wall itself. We tried to compensate for this as well. (figure 5.22)

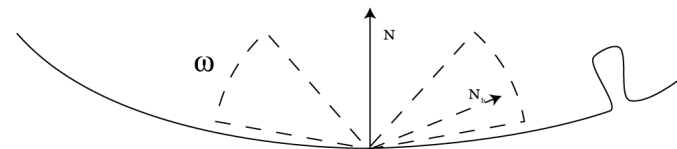


Figure 5.22 Ambient occlusion

We got best results with a maximum ray distance of 3 voxels. Figure 5.23 shows the ambient occlusion ratio with these settings. In figure 5.21, the ambient term in the lighting equation is multiplied by this ratio. Obviously, the more rays are cast, the less noisy the result is. For the visualizations in figure 5.23 and 5.24 we applied 128 rays per voxel which took about 5 minutes to render. As can be seen from the pictures, the algorithm successfully emphasizes the type details we are looking for, however when applied to the render it does not make a major difference. In other words, the algorithm does its job but the basic directional light used in our benchmark image does it better (figure 4.2, page 30).

5.2.3. Subjective assessment

We judge the techniques presented by their abilities to display different sized objects..

| | small objects | mid-sized objects | computational speed | consistent | intuitive | noise independent | flat lesions |
|-------------------|---------------|-------------------|---------------------|------------|-----------|-------------------|--------------|
| Viewforum | 0 | 0 | 0 | 0 | 0 | 0 | 0 |
| Strict shadowing | - | - | 0 | - | - | 0 | - |
| Ambient occlusion | 0 | 0 | -- | 0 | 0 | 0 | 0 |

It is clear that sharp shadows hide too many details and objects in the shadows. It does not provide the interaction between light and dark needed for a reviewer to better define shapes. Ambient occlusion proved to be unsuitable for the type of objects typically found in colons because of their organic shape, adding no shape information to the render. Moreover, the computational overhead is unacceptable, both when it is used in real time and using pre-computation.

5.3. Advanced shaders

The former algorithms all aimed to change the emphasis of the image by emphasizing details that were already in the image. Next we will try to communicate to the viewer some of what goes on behind the wall. We first implemented the relatively straightforward threshold projection, after which we tried a range of transparency techniques

5.3.1. Threshold projection

Our first attempt at showing the inside of the wall was based on the assumption that flat lesions contain a higher amount of muscle tissue (2.1.2). Showing this tissue in one way or another might invite the radiologist to further inspect the area. Because the flat lesion muscle tissue would reside close to

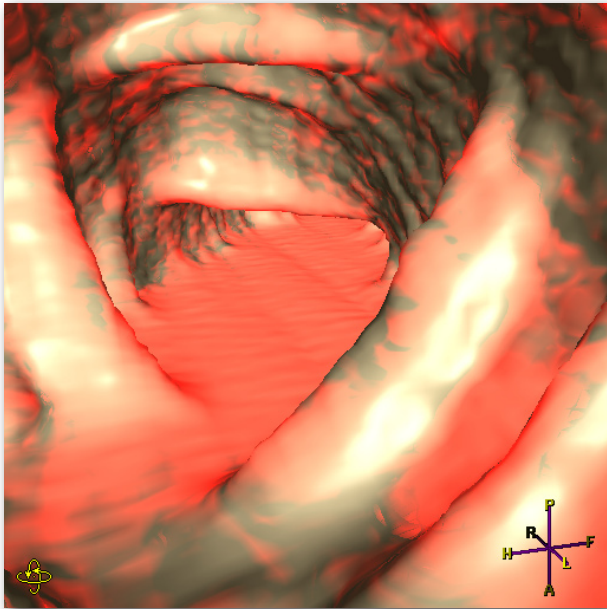


Figure 5.26 Threshold projection

the wall, we tried to probe the wall along the normal vector for a certain distance. Would the ray hit any fat tissue, the depth at which this tissue was found would indicate the amount of color that was added to the wall color (figure 5.25).

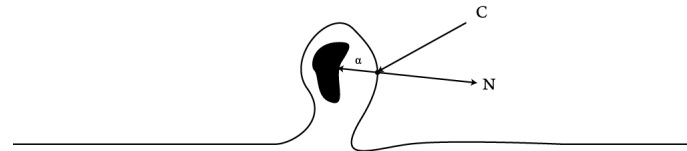


Figure 5.25 Threshold projection

As threshold value we choose 40 HU which is the theoretical value of the muscle tissue. As can be seen from figure 5.26, the results were not very promising. The algorithm suffers from a lot of noise that is being visualized which makes this technique unsuitable for material classification.

5.3.2. Transparency

An obvious next step in research towards the visualization of what lies beyond the colon wall is making the wall transparent. In order to do so, we need to define very clearly which HU values will be transparent and how much, and what colors are associated with those HU values. In the accompanying renders, we have done so as in figure 5.27:

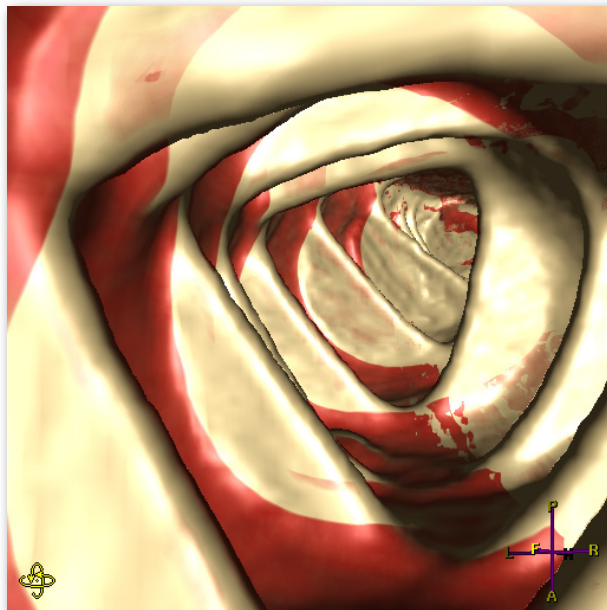


Figure 5.28 Transparency without falloff visualizes blood

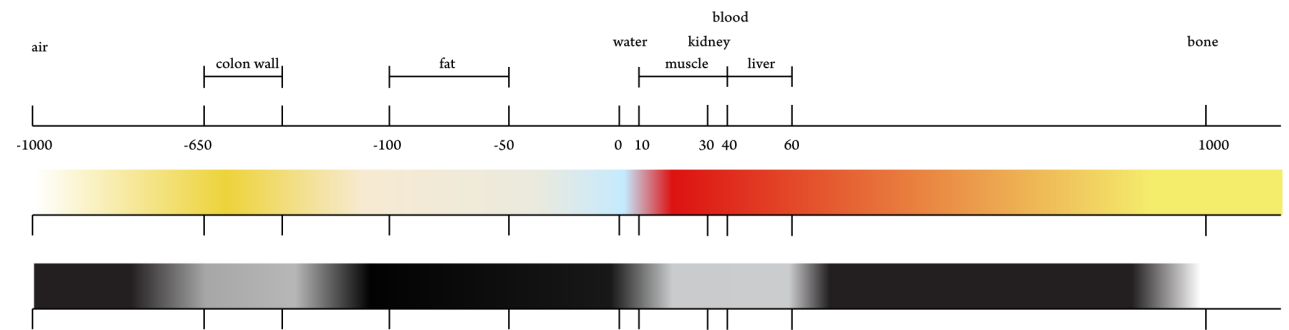


Figure 5.27. HU scale with associated colors and transparencies.

This scale shows that we made the colon wall partly transparent and muscle tissue slightly opaque. Note that the HU values for muscle, blood and various organs are very close together. Applying the transparency algorithm to the colon wall does not yield satisfactory results (figure 5.25). The main reason is that all blood and fat are visualized, both of which the area behind the colon walls are filled with. However, the tissue that we are looking for is located very close to the wall, which is why we applied a limit to the depth of the transparency probe. The depth (alpha in the picture below) is used as a factor

with the resulting color so that things further away from the wall will appear less prominently and not at all when further away than a certain depth (figure 5.29).



Figure 5.29 Depth-limited transparency

Although better, the algorithm still suffers from a lot of noise, something we try to tackle in the next paragraph (figure 5.30).

5.3.3. Transparency color mapping

By itself, the transparency algorithm is only marginally useful and worse, it clutters the render considerably. Using the transparency algorithm, it also becomes much harder to distinguish the shapes on the colon wall. Also, the radiologist will not be interested in what is going on behind the wall apart from the potential malignant areas. Therefore we moved back to the color mapping while keeping the positive aspects of the transparency tests. Color maps have the property that they do not violate the original shape perception; it is still possible to get a decent idea of the colon while conveying some extra information using the texture on the wall.

The example in figure 5.31 is a case where the muscle tissue in the flat lesion is very well separated. We found that this is usually not the case.

5.3.4. Subjective assessment

We assess the quality of the proposed techniques as follows.

| | small objects | mid-sized objects | computational speed | consistent | intuitive | noise independent | flat lesions |
|----------------------------|---------------|-------------------|---------------------|------------|-----------|-------------------|--------------|
| Viewforum | 0 | 0 | 0 | 0 | 0 | 0 | 0 |
| Threshold projection | - | - | -- | 0 | - | -- | - |
| Transparency | - | - | -- | 0 | 0 | -- | 0 |
| Depth-limited transparency | - | - | - | 0 | 0 | - | + |

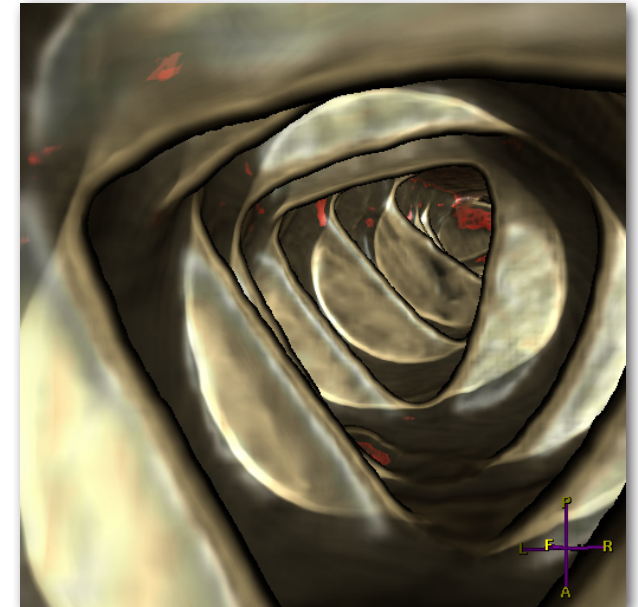


Figure 5.30 Transparency with a falloff of 5 voxels. Note how the muscle tissue inside the flat lesion stands out

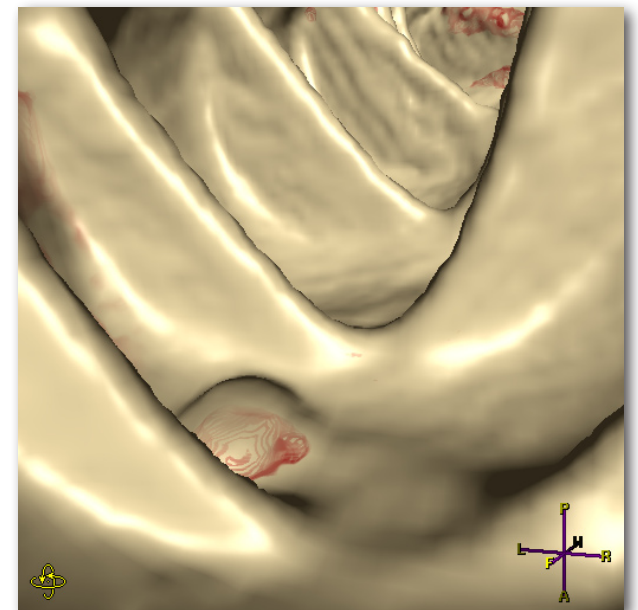


Figure 5.31 Transparency color mapping

| | small ob- jects | mid-sized objects | computa- tional speed | consistent | intuitive | noise inde- pendent | flat lesions |
|-------------------------------|--------------------|----------------------|--------------------------|------------|-----------|------------------------|--------------|
| Transparency color mapping | 0 | 0 | - | 0 | - | - | 0 |

All techniques attempting to visualize what lies beyond the colon wall with the aim to help provide information about potential lesions suffer from a common problem: the relatively large amount of noise behind the colon wall. Moreover, transparency considerably reduces the perception of the colon wall itself, thereby reducing the visibility of small and mid-sized objects. Transparency color mapping does not have this problem but is still very sensitive to noise. We will examine the depth limited transparency approach in more detail in the next chapter.

5.4. Conclusion

Although it is clear from current visualizations that the areas that grab a reviewers attention are fairly random (the emphasis is not well defined), shifting this emphasis to areas which are important proved to be quite a challenge. Some of our adapted lighting situations did not only not improve the visualizations, but decreased the amount of visualized details. The only technique that successfully shifts a viewers eye to different areas is the rim lighting. However, as it turned out the rim light emphasizes rims and small details (noise) in addition to other shapes, resulting in a cluttered image. Expert evaluation will be required.

The ambient occlusion did not help bring contrast at proper places. The main reason is the organic structure of the colon wall and the lack of sharp corners, to which the algorithm is sensitive.

The area behind the colon wall proved to be too noisy to be helpful towards the search for lesions without using specific features. The transparency visualizations showed too much blood, which is close in HU values to the muscle tissue present in lesions. Therefore, attempts to filter the area prior to visualization also failed. However, in the next chapter we will continue a variant of the transparency tests where we take focused features into account.

6. Feature dependent visualizations

The goal of the proposed enhancements is to assist the reviewer in finding polyps while examining the colon in 3D. In the previous chapter we tried to accomplish this by looking at general techniques that might shift the emphasis of the visualization towards more interesting areas. In this chapter, we focus more on the features that describe the polyps and try to enhance the render by incorporating those features.

Much research has been done towards features of polypoid lesions, which is why we rely on this research as much as possible. However, most research served a slightly different goal than we are after namely the detection of polyps. Where with detection algorithms the number of false positives is of utmost importance, in visualization this number is slightly less important especially if a measure of confidence can be attached to each candidate. This subtle difference sometimes made it worth re-implementing some feature detection algorithms.

Because flat lesion research is such a new topic, part of our work consisted of research towards the feasibility of the features that were reported for visualization. Radiologists define a flat lesion as an abnormal growth of tissue in the colon wall. Because of this extra growth, it is assumed that the colon wall is thickened at areas where a flat lesion resides. Furthermore, because of this extra tissue, slightly raised grey value levels can be observed in the orthogonal views. Moreover, there is the deformation of the colon wall. This last feature however is highly unpredictable, as can be read in the Background chapter and therefore unreliable for use as a feature. Lastly, some argue that villous adenomas have the tendency to hold contrast fluid (figure 6.1).

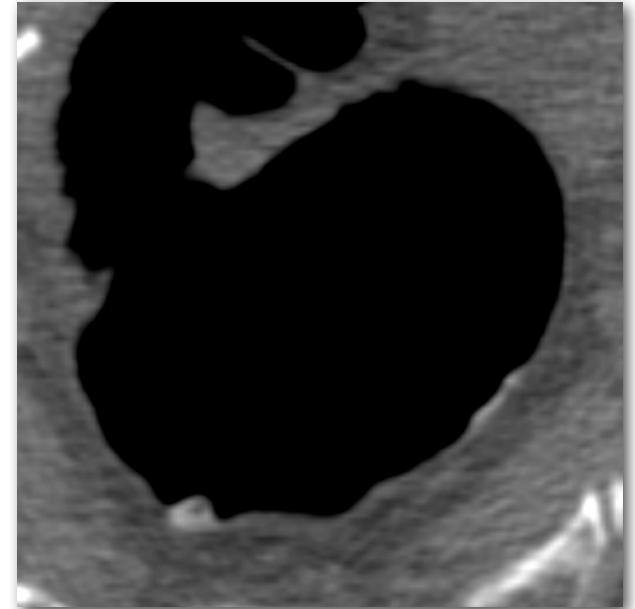


Figure 6.1 A flat lesion with contrast adhering to its surface

6.1. Candidate visualization

Some advanced research has been performed towards the detection of flat lesions. At the Physics department at the TU Delft, attempts have been made to classify flat lesions using statistical data features like mean values. None of it was successful enough to be viable for publication but most of it resulted in a list of potential candidates with their associated locations and confidence probabilities. We did some research towards the question whether these candidates can be visualized in a sensible way.

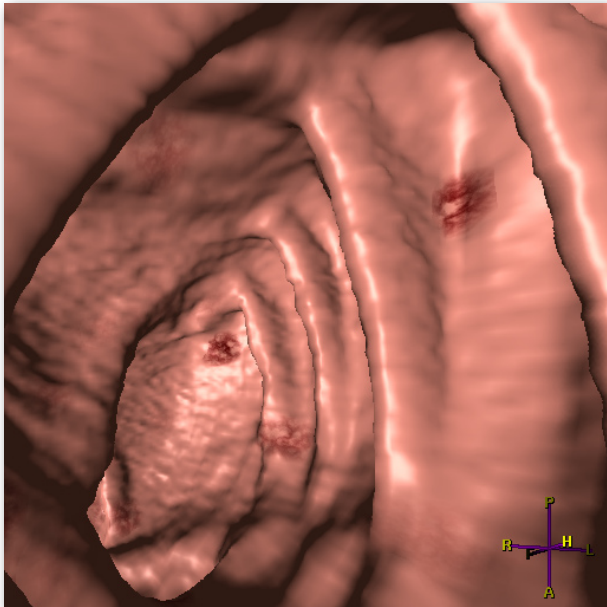


Figure 6.2 Realistic candidate visualization

6.1.1. Realistic rendering

The first attempt consisted of a realistic render of the candidate in question. Realistic rendering is the attempt to visualize the lesions as realistically as possible using the information in the CT scan, thereby mimicking what a radiologist sees during an optical colonoscopy. Rendering realistically is not widespread accepted because it might possibly suggest suspicious areas to the reviewer in places where there is nothing wrong. Nevertheless we implemented an algorithm that mimics real polyps to some extent (figure 6.2).

As can be seen in transcript movies from optical colonoscopy, most polyps have a reddish color with slightly darkened veins. To determine which parts of the colon wall should be colored, we define a standard polyp size. The part of the colon wall surface that is within the area defined by the sphere around the candidate is assigned the deviating color.

In order to get a sense of realism, we implemented a Perlin noise generator [Perlin 1985]. A Perlin noise function is essentially a seeded random number generator. Based on a seed number it always returns a random number which is the same for every time the function is called with that number. By interpolating between these numbers a gradient function is acquired, and by adding different versions of the number generator (differing in amplitude and frequency) we end up with a random pattern that is very suitable for mimicking fluids and streams in computer graphics.

A typical polyp shows very small veins on the surface of the polyp. A Perlin noise generator returns values between -1.0 and 1.0, and by applying the following formula and using the result as a measure for the intensity of the veins we are able to produce something that looks like the real veins:

$$c = 1.0 - |p|$$

How this function works can best be explained when we interpret the Perlin noise as a standard sine function, which it resembles (figure 6.3a). The example is 1D although we use the 3D version.

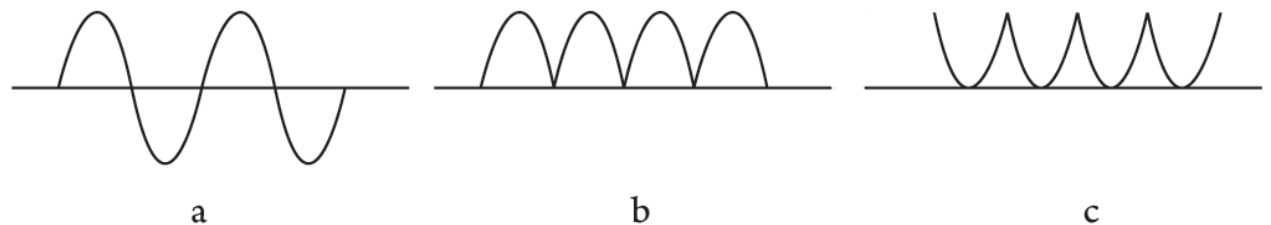


Figure 6.3 Retrieving the red color based on the perlin noise generator

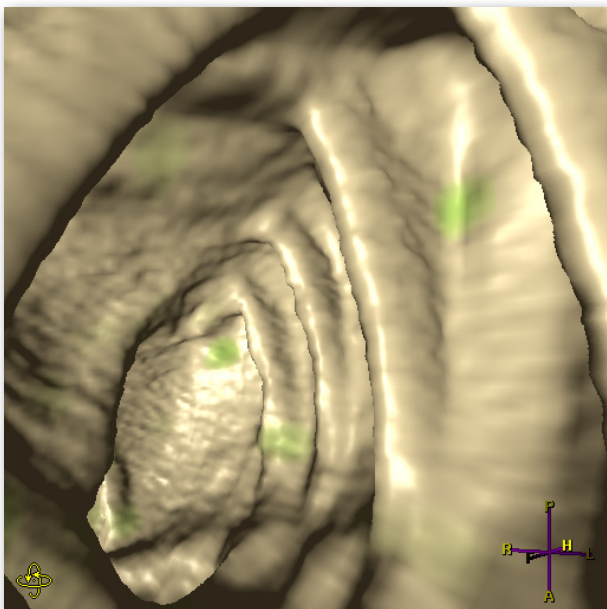


Figure 6.4 Meta color candidate visualization

First, we take the absolute value of the function (figure 6.3b), which introduces sharp knits when the function goes to zero. By inverting the result, we get sharp peaks near 1 and gradual valleys near zero (figure 6.3c). The result is a measure for the amount of red color near a candidate and defines the typical looks of veins (figure 6.2). Next, the candidates come with a probability that indicates the confidence of a candidate. This probability is a cumulation of all other factors that were researched. This probability is multiplied by the factor we calculated earlier, to ensure that candidates we are less sure about appear less prominently. The size of the visualized lesion is predefined.

We could probably improve this result but there are a couple of serious issues with this approach. The biggest problem is that the information we are visualizing differs from the message that is displayed. The information we have is the confidence that something that has the features of a polyp exists at that location, and what we are visualizing is the strength of a polyp (that we show does exist at that location). Obviously, these factors can differ considerably. This reason alone is a strong argument that using realistic colors is not a good choice.

6.1.2. *Meta color maps*

A couple of variations of the aforementioned algorithm were attempted. We replaced the Perlin noise generator with a color (figure 6.4). However, as it turns out the number of candidates is still too high, and the colors lose their value quickly.

We also attempted one more subtle effect. By changing the lighting slightly at the location of the candidate we were able to shift the focus to the candidates somewhat more. However, the problem of the suggestive nature of candidate visualization remained.

6.2. Curvature visualization

Current polyp detection algorithms use curvature information to find polyps. There are two ways to get an estimate of the curvature. The first is developed by Yoshida et al. and uses a shape index in combination with the curvedness index [Yoshida et al. 2002] This method was discussed in detail in the 3.1.2. The curvature and shape indexes can be calculated for every voxel in a volume, which implies they can be pre-calculated. Both indexes can be applied directly to a visualization algorithm. The second method was also discussed in the Previous work and uses curvature streamlines to generate a representation of the streamlines. Most of our tests are based on Yoshida's work.

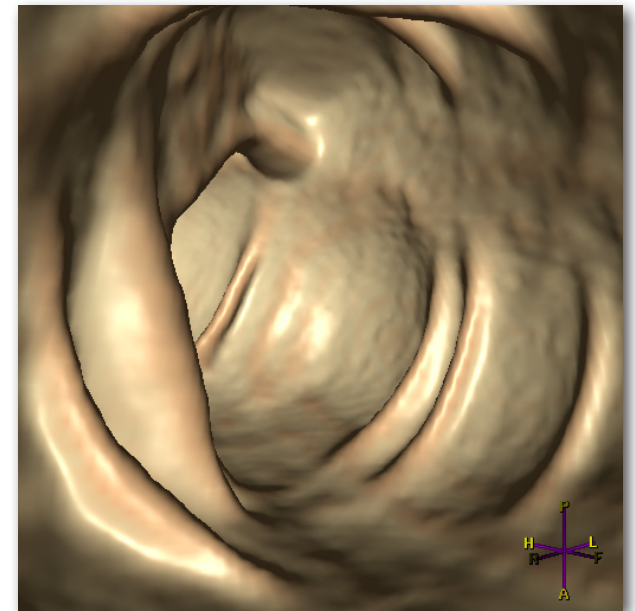


Figure 6.5 Shape index visualization: more red means higher shape index

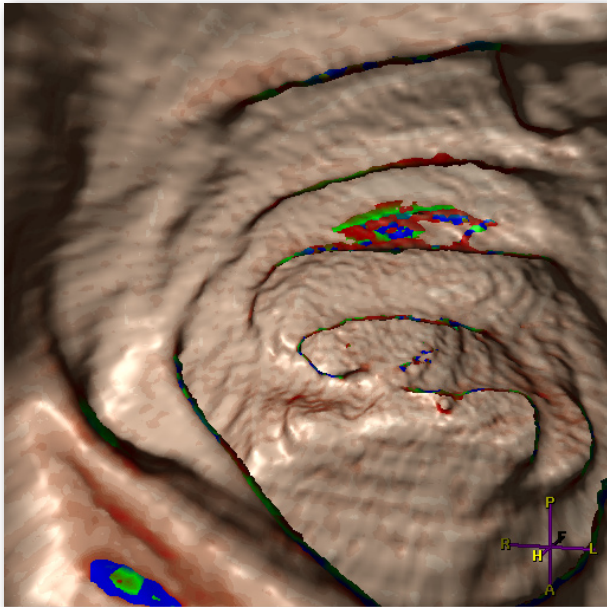


Figure 6.6 Wall thickness visualization. The green, red and blue colors mean deeper areas.

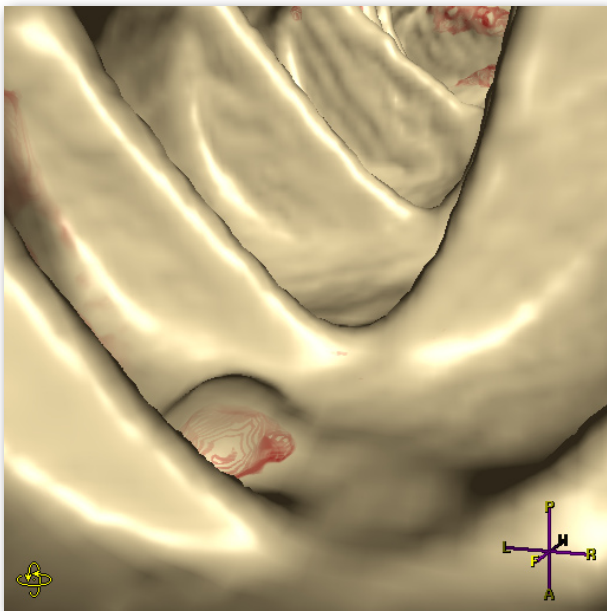


Figure 6.7 Blood visualized

Figure 6.5 shows the effect of applying the curvature as a color to the render. It turns out that the curvature and shape index information are great features for detecting polyps but that there are serious issues with them during visualization. Firstly, when shapes transform from one shapes to another, they cross a lot of other shapes, which in turn means a lot of response from the visualization algorithm. In figure 6.5 one can see that the reddish color (which means a high shape index and is typical for polyps) is visible at the top of the folds as well as all other surfaces that protrude from the wall. Secondly, it is not clear to the untrained eye what the colors mean. A radiologist typically has no experience with the subject matter. The visualized information therefore will be of limited use to him or her.

The curvature visualization can possibly be improved by applying the curvature information in a more sensible way. By combining the shape index information with the curvedness, it might be possible to emphasize areas that have the shape of polyps by coloring those areas slightly different. Yoshida reports good results which is why this information is likely to work in visualizations as well. More research is possible towards this technique.

6.3. Wall thickness

As a first test, we attempted to visualize the wall thickness by probing the colon wall until we reach a predefined value. Obviously this cannot yield a usable result because the colon wall does not have a constant grey value level at the location of the flat lesion. However, we still performed some tests to see how the algorithm would behave. One thing that is immediately evident is the fact that the colon wall thickness is not constant even at locations other than flat lesions. The folds present in the colon consist of the same intensity as the colon wall. This results in the fact that the top of the folds are interpreted as thick colon walls, as can be seen in figure 6.6. The algorithm did not respond to the flat lesion in the upper right corner.

Because of these disappointing and unpredictable results, we stopped experimentation with the colon wall thickness in an early stage.

6.4. Raised grey value level

A feature that is present in most flat lesions we have studied is the raised grey value level. However, the difference between the values inside the flat lesions and the surrounding colon wall tissue and the organs behind the colon wall is fairly small. The theoretical highest value is around 30-40 HU. However,

because of scanner limitations, lesions tend to have a highest value of approximately 20 HU which is about 20 HU higher than the area behind the wall. Much lower high values have also been spotted. Another problem is that the variation of the noise is fairly high behind the colon wall. Furthermore, the flat lesions is not the only thing that has a raised grey value level. Behind the colon wall blood and organs are found that have approximately the same HU values. All these factors cause this feature to be potentially unreliable.

6.4.1. *Transparency revisited*

In order to see exactly how feasible this feature was, we applied our transparency algorithm from the previous chapter to the colon and adjusted the opacity scale to show the colon wall and the HU values we are after.

2D filtering parallel to the colon wall

To reduce the influence of noise, we applied filtering before testing the values against the opacity scale. In order to avoid the influence of the lumen on the filter, we used a 2D filter that is aligned parallel to the colon wall. This is achieved by rotating the filter so that aligns with the plane orthogonal to the surface normal vector. Because of the anisotropic properties of the data, the filter will also have to be anisotropic, a fact we ignored for now. All filters are centered around the location to be filtered. The filter is applied along the ray path when tracing the ray into the wall, and the result is used as input in the transparency algorithm.

Our first filter consisted of a simple 3x3 mean filter. By mean filtering we expected we could smooth the noise while maintaining some of the flat lesion because the flat lesions usually are larger than the noise chunks. As it turns out, averaging with a 3x3 filter already lowers the highest HU values so much that the flat lesions are almost erased.

A second filter consisted of a Gaussian filter, applied in the same way as the mean filter. Gaussian filters have the advantage that they provide gentle smoothing. For us, the main advantage is that it weights the center pixel more heavily than the surrounding pixels. Although this will also better preserve the noise, we expect the averaging effect of the filter to be stronger near noise spikes since the area around a flat lesion gets lower more gradually than the area near a noise spike. In other words, the Gaussian filter is expected to make the data more predictable. We chose a filter size of 5x5 and a sigma of 2.0, which ensured the filter would be zero near the edges and would climb evenly near the center of the filter.

Unfortunately, even after the filtering, we did not get convincing results (figure 6.7). The presence of blood in the colon wall considerably disturbs the visualization. The main problem is that a blob of

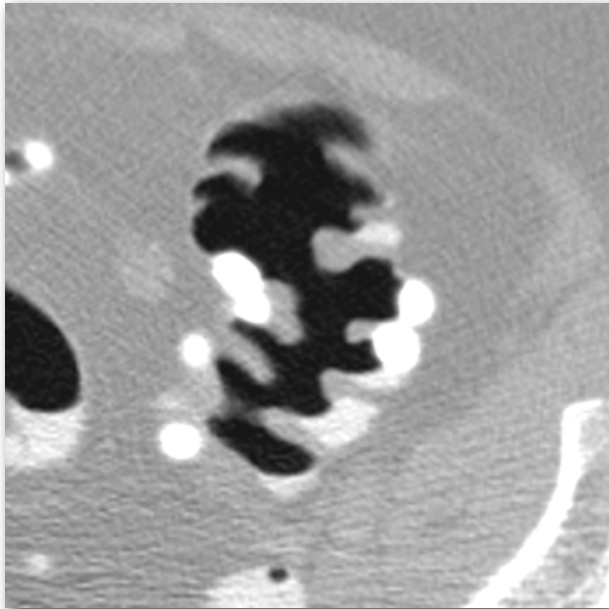


Figure 6.9 Some examples of dilated areas. The white blobs represent the raised HU values

blood has almost exactly the same HU value as occurs in the flat lesions, and typically has the same size as flat lesions. This makes flat lesions very hard to extract.

6.4.2. Flat lesion dilation

The transparency algorithm proved to be very sensitive to noise, even after various filters were applied. To improve the results, an algorithm is needed that would not visualize individual high grey value voxels, but would respond to the small clusters located closely to the colon wall.

The idea of dilating flat lesions is based on the displacement of the colon wall at the location of the flat lesion depending on the raised grey value levels (figure 6.8).



Figure 6.8 Displacing the colon wall at the location of the flat lesion

Displacing the location of the iso-surface itself based on raised HU levels behind the iso-surface would involve some heavy computations and therefore unsuitable for practical use. However, an easier way with approximately the same result would be to dilate the flat lesions in advance of the actual computation of the iso-surface. The idea is to raise the HU values in the proximity of a high HU value in the colon wall. Figure 6.9 shows an intersection of the colon wall near a flat lesion (F). Every voxel in the colon wall mask is thresholded against 100 HU. For all remaining voxels a Gaussian function is centered around these voxels, after which the function is added to the image at that location. The reason we use a Gaussian function is to avoid aliasing effects; the smooth transition of the function from its top to the edges in a circular manner ensures that the iso-surface will be displaced smoothly as well.

The method resembles a convolution but instead of multiplying the function, we add the function. We could have used a multiplying filter as well, but using an addition gave us some additional flexibility. In the first place it allowed us to use a straightforward Gaussian for which the result is easy to predict. Secondly, it allows more refined thresholding methods, which we will need in the next paragraph where we will apply a connected component analysis to the mask. Thirdly, because we can apply a mask we will only have to apply the function to the voxels that are in the colon wall mask, which improves the performance of the algorithm considerably.

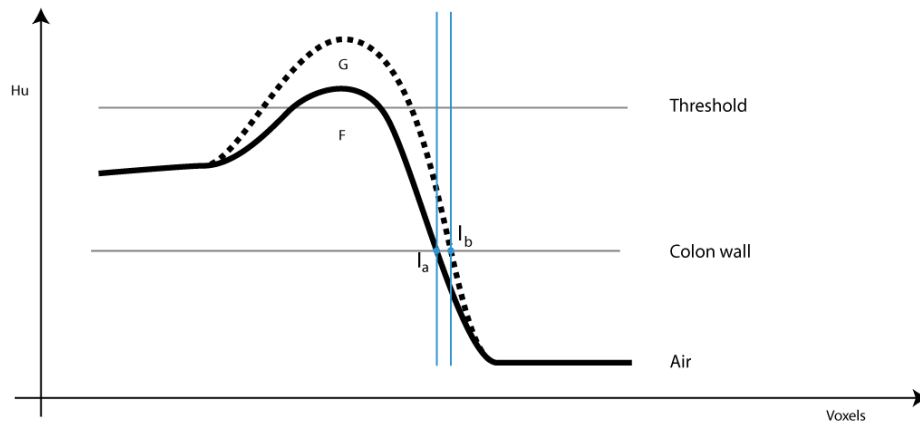


Figure 6.10 Dilating flat lesions

As can be seen in figure 6.10, adding the Gaussian function results in higher HU values at the location of the iso-surface (the blue line), which in turn displaces the iso-surface from I_a to I_b .

The algorithm is executed in three steps. First, a layered representation of the colon wall mask is obtained. Next, these masks are used to filter the image which is necessary to reduce the effect of noise on the result. Lastly, the actual dilation is performed.

Obtaining the colon wall masks

Because CT data sets usually consist of heavy noise behind the colon wall, we need to apply a filter. In order to get an optimal result that is not influenced by the lumen, we need to filter parallel to the colon wall. Therefore, we need a layered mask representation of the colon wall. First, the mask of the colon lumen is extracted by applying a threshold of -650 HU values where everything lower than the threshold is assigned 1 and higher 0. Next, this mask is dilated a predefined number of times with interchangeably a 8 and a 4 connectivity filter. Interchanging 8 and 4 connectivity filters will result in masks that more accurately follows the original lumen mask. After each dilation, we perform a binary subtraction with the previous mask in order to obtain only the dilated part. Every result of this operation is stored separately. We discard the mask of the lumen. Combining all layer masks would give us an accurate mask of the colon wall including potential flat lesions (figure 6.11).

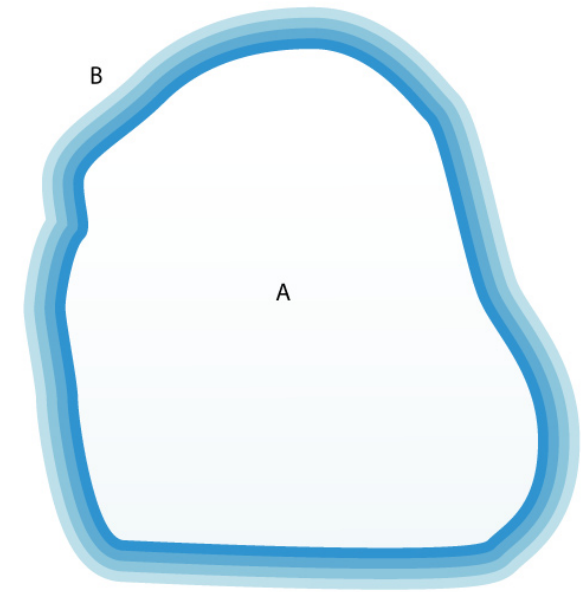


Figure 6.11 Layered colon wall mask: a) Colon lumen b) Layered masks

1) This is based on experience at the Philips Medical Systems research center.

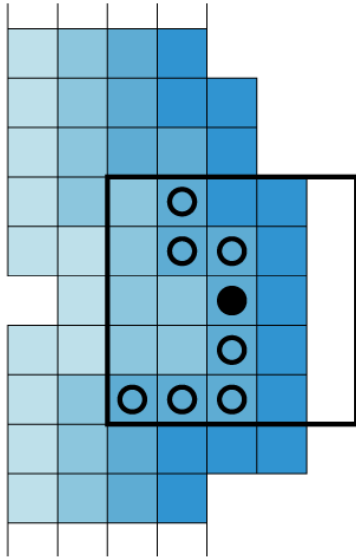


Figure 6.12 Filtering the colon wall using a 2D mask

Mean filtering

The second step is the actual mean filtering. We define a mean filter with coefficients that add up to one which means that for a 5x5x5 filter the coefficients are 0.008. For every pixel that is in on of the colon masks, we apply a convolution of the filter with the original grey value image [Gonzalez et al. 2002]:

$$f(x, y, z) \star h(x, y, z) = \frac{1}{MNO} \sum_{m=0}^{M-1} \sum_{n=0}^{N-1} \sum_{o=0}^{O-1} f(m, n, o)h(x - m, y - n, z - o)$$

where f and h are the images to be convolved and M , N and O are the sizes in three axial directions of the images. The filter is zero for every pixel but for a cube in the center of the image. The size of this cube defines the filter size.

If we simply apply the 3D mean filter, the result will be biased because it will suffer the influence of the lumen. Therefore, we mask the filter with the corresponding mask layer we calculated in the first step. This mask follows the shape of the colon wall which ensures the filter will only be affected by the colon wall and not by the lumen

The filtering is done in a four-step process. For every voxel in the masks we calculated earlier:

1. Find the mask the current voxel is in.
2. Center the 3D mean filter on the current voxel
3. For every pixel in the filter, find the corresponding value in the mask and multiply the filter with the mask. This results in a masked mean filter. In figure 6.12 the result of this step is shown; the closed circle represents the current voxel, and only the pixels with open circles will be used in the filter.
4. The filter still needs to add up to 1, so the values of the pixels in the filter are reassigned. The pixels where the mask is 1 are set at 1 divided by the number of pixels in the mask, and 0 where the mask is 0. For example, the values of the pixels in the mask in figure 6.12 (the circles) are $1/8 = 0.125$ and 0 otherwise.
5. Multiply the resulting mean filter with the image and add the results. This results in a mean value which is the new value for the current voxel.

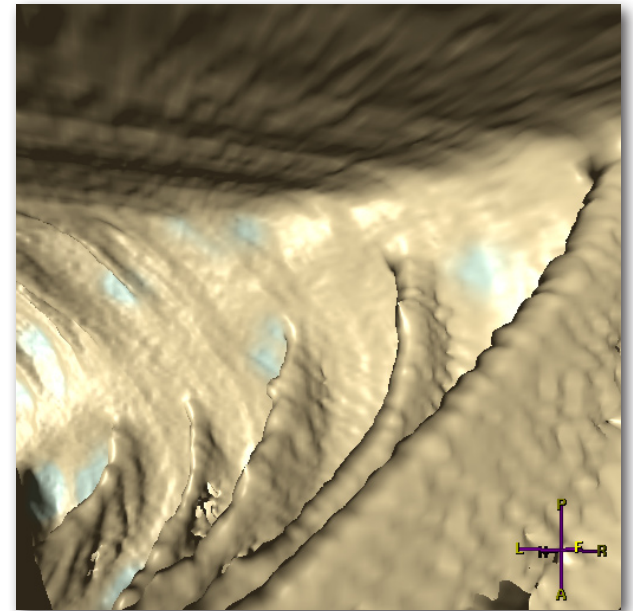
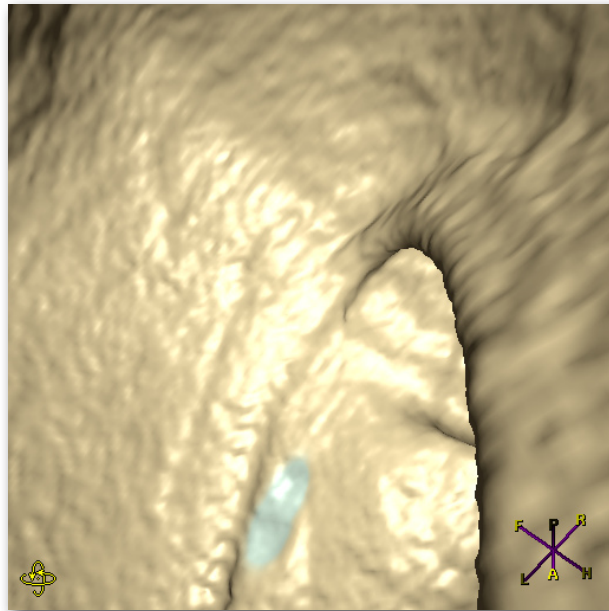
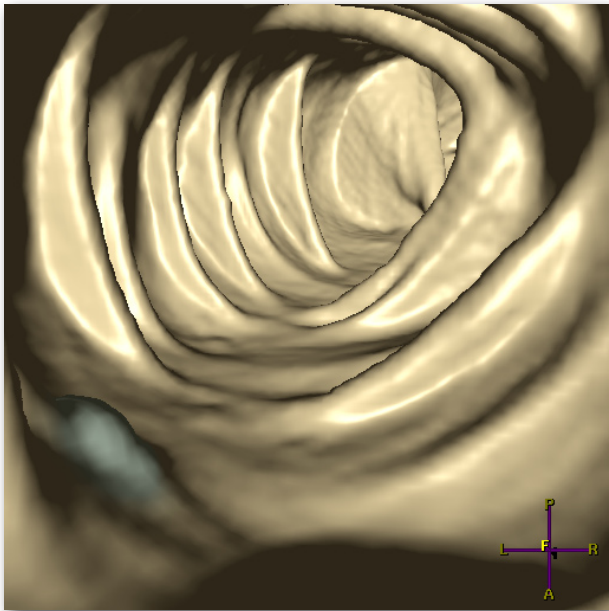
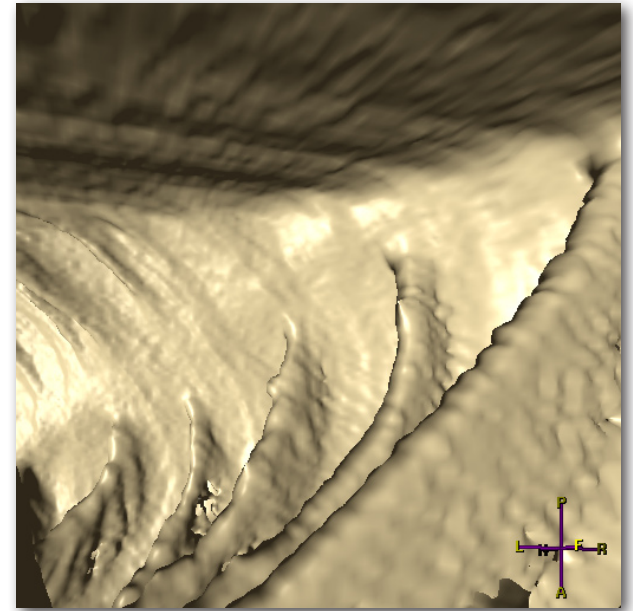
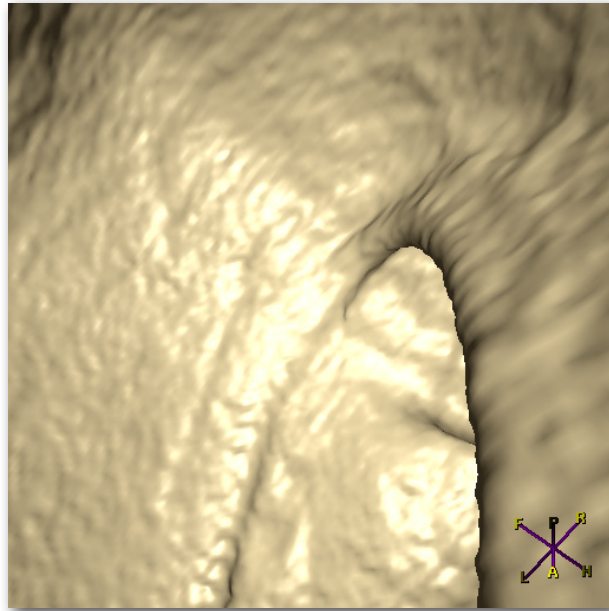
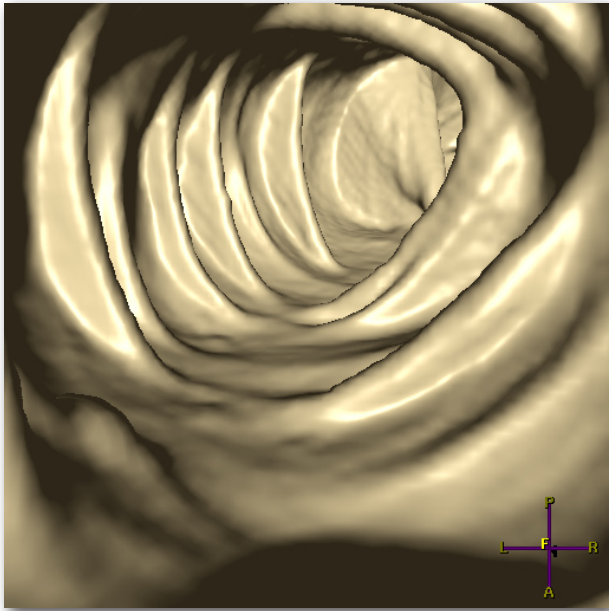


Figure 6.16 Flat lesion in descending colon a) original render b) dilation coloring

Figure 6.17 Flat lesion in rectum a) original render b) dilation coloring

Figure 6.18 Example of a location where small clusters of contrast sticking to the colon wall form false positives

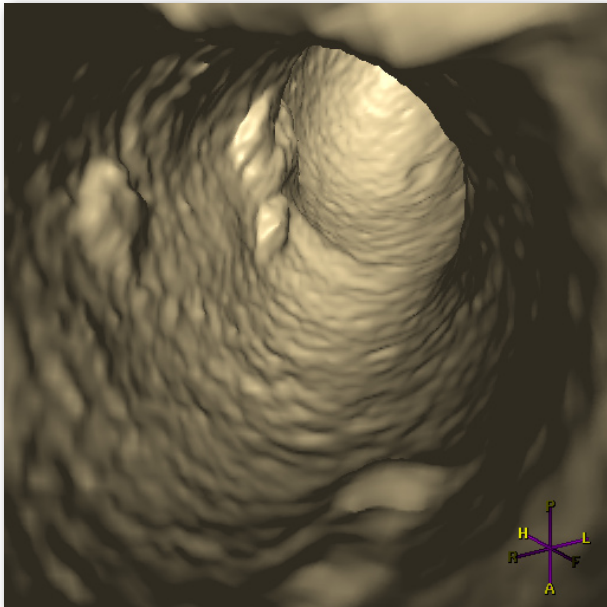


Figure 6.13 The dilated flat lesion. The flat lesion in the front is correctly dilated but a lot of noise has been dilated as well.

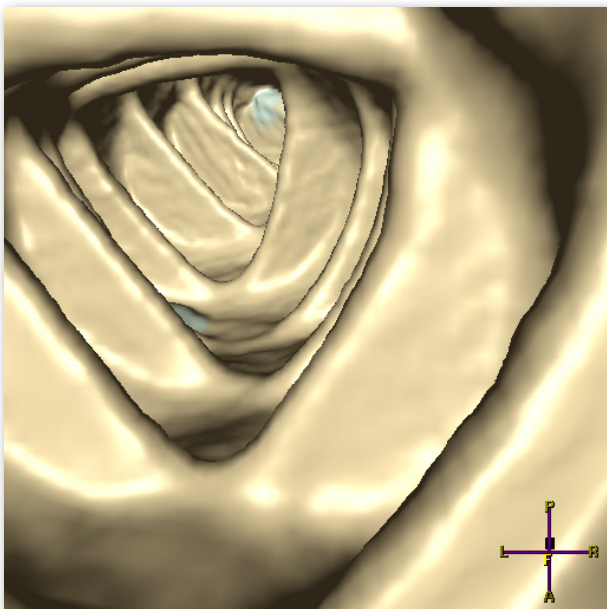


Figure 6.14 The dilated areas are colored

This results in a 3D image that is filtered parallel to the colon wall.

Dilating the flat lesion candidates

The last step is the actual dilation of the data set (figure 6.12). Every voxel in the image that is in the colon wall mask and in the contrast mask calculated in step 2 is thresholded against a predefined value. If the value is higher than the threshold, the filtering is applied, else this step is skipped. Again, a filter is defined. Defining a filter with equal coefficients results in considerable aliasing effects, which is why we define a Gaussian filter. The filtering does not consist of a multiplication step like usual when convoluting a volume. Instead, we center the filter on the pixel to be filtered and add the filter to the volume at that location. This lifts the grey values around the flat lesion candidate, thereby displacing the iso-surface (fig 6.9). As discussed previously, a normal convolution would have been possible as well.

We got best results when mean filtering with a masked 5x5x5 filter. Although the spikes found in flat lesions were reduced, the reduction was less than found at noise spikes, resulting in a more predictable pattern. For dilation we used a 9x9x9 filter with a sigma of 2.3 which we multiply with 1000. This results in values of 450 near the center and almost 0 near the edges of the filter. The chosen sigma is dependent on the size of the filter and ensures a smooth ascent in value towards the center in this case. The filter size is based on data sets of 512x512x500 voxels which equals approximately 400x400x450 mm. This inherently means the filter is anisotropic, which we did not consider to be a major problem.

In order to be able to judge our algorithm more accurately, we also visualized the displacement of the new colon wall on the original colon wall by subtracting the two volumes and using the result as input for the color of the colon wall (figure 6.14). This resembles the visualization of contrast fluid which we will discuss in the next paragraph.

The algorithm works as expected but as can be seen in figure 6.13, the algorithm suffers from many false positive dilations. The false positives are generated by nearby blood and stool, as well as larger spikes of noise.

6.5. Contrast fluid sticking to lesions

Some literature claims that contrast fluid has the tendency to stick to certain types of lesions [O'Connor et al. 2006]. The theoretical value of contrast fluid lies between 300-400 HU. Due to the partial volume effect and noise, we found maximum values between flat lesions between 100 and 400, which is still distinctive enough to be useful. See Appendix A for an overview of our reference data.

We adjusted the algorithm in the previous paragraph and applied it to the data (figure 6.14). Because the HU values of contrast fluid are considerably higher than flat lesions and the fact that contrast fluid sticks to the wall instead of residing inside the wall, we found that mean filtering prior to the dilation only degraded the results because of the influence of the lumen even after applying the layered mask filter. Instead, we apply a connected component analysis on the mask of the high values in the colon wall.

6.5.1. Obtaining the small cluster contrast mask

In order to obtain a mask of the small clusters that possibly represent flat lesions, we first thresholded the image to obtain objects with a HU value higher than 100 HU. We applied a binary AND operation with the mask obtained by dilating a mask of the lumen six times, which results in only the high value objects in the colon wall. In order to remove large clusters that represent contrast fluid pools, we applied a modified version of the two-pass connected component analysis as described by Shapiro and Stockman [Shapiro 2002]. This is done as follows:

1. For every voxel that is in the colon wall mask and is not the background:
 - Find all labeled neighbours. If no labeled neighbours are found, assign a new label to the current voxel. If labeled neighbours are found, assign the lowest label to the current voxel.
 - Keep track of equality with other labels in the neighborhood in order to be able to define which clusters are the same cluster. For example, when we find a voxel with 2 neighbours that have labels 3 and 5, we assign the label 3 and we remember that labels 3 and 5 belong to the same cluster.
 - Keep track of the amount of times every label is assigned
2. For every label that belongs to the same cluster, add up the number of times the labels are assigned. This results in the cluster size for every cluster.
3. Loop through the colon mask again, this time assigning 0 to any pixels that belong to clusters larger and/or smaller than a predefined amount of voxels

Shapiro et al. define a secondary loop through the mask (hence the name two-pass) to assign the lowest equivalent label to the clusters. This is not necessary in our case because we are not interested in the clusters themselves but only in the size of every cluster. Because we know the size of the cluster and all labels that are associated with the cluster, we know which labels we can eliminate.

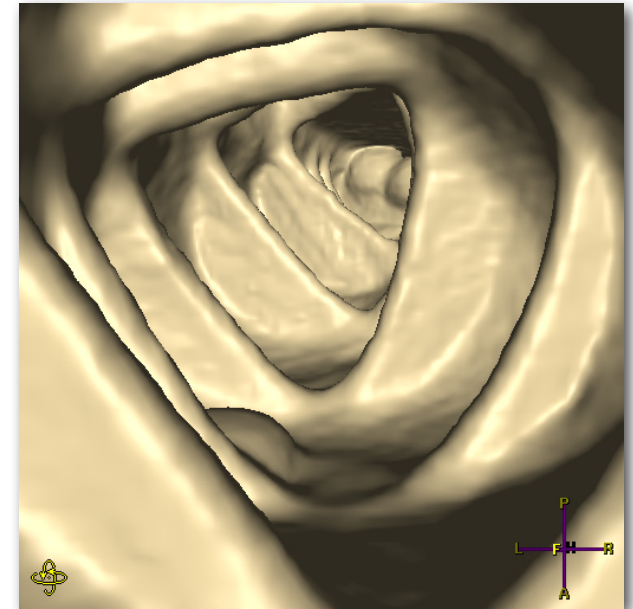


Figure 6.15 Dilated contrast fluid. Notice how sticky contrast in the back gets dilated as well

The resulting mask defines which pixels are dilated. We found the ideal size of the clusters to be between 20 and 100 voxels based on our data (Appendix A). Most flat lesion fluid films lied well within this range. The clusters that were selected apart from the flat lesion were either small pools of fluid pulled down by gravity, or structures that look very much like flat lesions.

Again we evaluate the dilation using a coloring technique in order to be able to see more clearly what the effects are. Results are evaluated in more detail in the next chapter but for now we can state that results differ from patient to patient and is largely dependent on the amount of remaining feces. There are occasions where there are only 3 areas colored per colon of which one area is a true positive flat lesion (figure 6.16 and 6.17). In other cases, the number of false positives rank between 20-30 colored areas. Figure 6.18 shows a bad case where small pools of contrast are taken as candidates. No flat lesion with attached contrast fluid is missed in the data sets we used.

Because small cluster contrast coloring can be ambiguous in what one sees we also did tests with the algorithm without removing large clusters (figure 6.19).

6.6. Conclusion

We summarize our conclusions as follows.

| | small objects | mid-sized objects | computational speed | consistent | intuitive | noise independent | flat lesions |
|-------------------------|---------------|-------------------|---------------------|------------|-----------|-------------------|--------------|
| Viewforum | 0 | 0 | 0 | 0 | 0 | 0 | 0 |
| Candidate visualization | 0 | 0 | 0 | 0 | -- | 0 | - |
| Curvature visualization | 0 | 0 | 0 | 0 | - | 0 | 0 |
| Wall thickness | 0 | 0 | 0 | - | - | - | - |
| Dilated flat lesions | 0 | 0 | 0 | - | + | - | + |
| Colored dilation | 0 | 0 | 0 | - | + | - | + |
| Colored contrast fluid | 0 | 0 | 0 | + | + | + | 0 |

The candidate visualization is problematic because it is inevitable that one judges certain areas of the colon wall with the visualization. Another problem is that the candidate list is still far too long resulting in too many false positives even for visualization. Candidate visualization may be feasible when the detection is improved, but it is likely that direct application of the feature calculators to the visualization will be more effective because this does not limit the visualization to the location of the candidate.

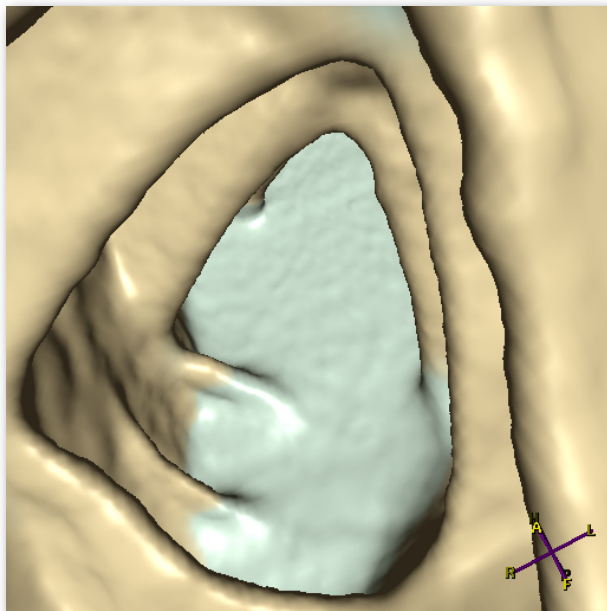


Figure 6.19 A pool of feces and contrast fluid

The curvature visualization can certainly help shift focus if some additional research is performed. However, it is uncertain that shifting this focus will result in more found polyps. Extensive research with a multitude of radiologists and data sets would have to be performed

The dilation of the flat lesions resulted in the most interesting results. It proved too difficult to visualize the assumed high values inside flat lesions because of the excessive amount of similar structures like blood, stool and organs. However, when introducing the assumption that contrast fluid tends to stick to flat lesions, the results improved because contrast has much higher HU values, making it easier to distinguish the contrast film. This reduced the number of false positives considerably.

Now that we have presented all the techniques that we tested, we will evaluate some of them in the next chapter using expert evaluations.

7. Expert evaluation

Some techniques described in the previous two chapters looked promising enough to be evaluated by radiologists. We decided to perform focused interviews with experts from Amsterdam Medical Center to evaluate our findings. We first defend the choice of the evaluated techniques we chose, after which we introduce the used evaluation method and lastly the results.

7.1. Proposed techniques

Unfortunately it proved to be very hard to enhance the visualization in a sensible way while not using any features. The only technique that successfully shifts attention to potential malignant areas is the rim light technique. Visualizing features proved to be just as hard when looking at flat lesions. However, the dilation algorithms and their derivatives looked promising enough. Because it is mainly contrast that we are visualizing we also include the contrast visualizer without the removal of large clusters. We summarize our own subjective conclusions below.

| | small objects | mid-sized objects | computational speed | consistent | intuitive | noise independent | flat lesions |
|------------------------|---------------|-------------------|---------------------|------------|-----------|-------------------|--------------|
| Viewforum | 0 | 0 | 0 | 0 | 0 | 0 | 0 |
| rim lighting | + | + | 0 | - | 0 | - | + |
| dilation | 0 | 0 | 0 | 0 | - | - | + |
| dilation coloring | 0 | 0 | 0 | 0 | - | 0 | + |
| contrast visualization | 0 | 0 | 0 | 0 | + | 0 | 0 |

7.2. Evaluation approach

Our experts consisted of multiple radiologists that have screened at least 500 colons each. All experts were attached to the Amsterdam Medical Center. Evaluation was executed based on individual interviews. For every technique we asked the experts to assess the quality of the proposed techniques based on the following criteria, all ranked on a scale from - - to + +. As assessment material we showed

them side by side movies of the original renders and the application of the new technique. For every technique, we tried to pick movies that accurately represent the average results.

7.2.1. *Reviewing speed*

Reviewing speed measures the speed at which a reviewer is able to work his way through a colon. Reviewing speed is important because radiologists typically need to look at a lot of colons in a row and longer reviewing speeds might decrease their accuracy.

7.2.2. *Lesions found*

Increasing the number of found lesions is the ultimate goal. This can be done directly by showing the radiologists the (features of) the lesions, but also indirectly where we show features that indicate the presence of a substance for example, that may help the radiologist draw certain conclusions

7.2.3. *Esthetic value*

Although not the most important, esthetic value can increase the sense of reliability of a system. If a system has professional looks, a user tends to trust the system which has become an important factor in modern software.

Because the interview resulted in detailed discussions about the choices and recommendations of the experts, we include a summary of these discussions where applicable in the results.

7.3. Results

The results of our interviews are as follows. As pre assumptions we asked the radiologists to assume that the 3D visualization would be his prime method of inspection, as opposed to scrolling through 2D slices and occasionally inspecting the 3D viewer.

7.3.1. *Rim lighting*

| | speed | number of found lesions | esthetic value |
|--------------------|-------|-------------------------|----------------|
| Senior radiologist | 0 | 0 | - |
| Junior radiologist | 0 | 0 | 0 |

The senior radiologist did not believe the rim light would add major value to the render. He found it hard to assess the value because his prime inspection method is the orthogonal view. He agreed that the rim light does show some extra details that would otherwise be hidden but it mainly targets small variations and does not make any difference when it comes to either speed or the number of found

lesions. Moreover, the radiologists had a slight preference for the original renders for esthetical reasons, mainly because of his extended experience with the original renders. He stated that this would probably be the main reason for his preference and that it would probably only be a matter of days to get used to.

The junior radiologist was slightly more positive. She appreciated the fact that more detail was visible in the render although she felt that the lighter rims made the flat lesions blend in more. She did not think this technique would considerably change the speed or the number of found lesions.

7.3.2. Dilation

| | speed | number of found lesions | esthetic value |
|--------------------|-------|-------------------------|----------------|
| Senior radiologist | -- | + | 0 |
| Junior radiologist | - | + | 0 |

The senior radiologist appreciated the idea to dilate flat lesions. He thought that this technique might increase the number of flat lesions when 3D visualization would be the prime screening method. However, it would also decrease the reviewing time due to false positive findings. He considered the introduced bias to be a problem.

The junior radiologist believed that this technique could increase the number of found lesions as well, but also recognized the extra time involved. She also felt that a great number of false positives (> 15) might deceive the reviewer into ignoring the dilations.

7.3.3. Dilation coloring

| | speed | number of found lesions | esthetic value |
|--------------------|-------|-------------------------|----------------|
| Senior radiologist | -- | + | 0 |
| Junior radiologist | - | + | 0 |

The senior radiologist felt that the idea to mark regions of interest is a good idea. However, coloring the flat lesion candidates will cost more time. He remarked that this might be especially beneficial to unexperienced readers. He also remarked that he could not confirm that contrast does stick to flat lesions.

The junior radiologist stated again that it would be a serious problem if there were too many false positives because of the risk of ignoring them.

7.3.4. Contrast coloring

| | speed | number of found lesions | esthetic value |
|--------------------|-------|-------------------------|----------------|
| Senior radiologist | - | 0 | 0 |
| Junior radiologist | - | 0 | + |

The senior radiologist felt it would be especially important for this technique to be helpful that the patient would be prepared correctly, which is usually not the case. Excessive amounts of fecal residue would degrade the value of the contrast considerably. He found it hard to assess the value of contrast coloring because of his extensive experience with the orthogonal views as a prime method, where it is immediately obvious what is contrast and what is not.

The junior radiologist was more positive and appreciated the visualization of contrast. However she mentioned that if all fecal residue is colored, a polyp might be easily judged as residue because of the color, and thus discarded.

7.4. Preliminary conclusions

We will present our conclusions in the next chapter, but solely based on our interviews we can already conclude a number of things. The radiologists found not much use for the rim lighting technique. Although they acknowledged that it slightly enhanced what they saw, they did not recognise that it is enough to change what they already have.

It is unsure that adhering contrast fluid is a correct feature. However, assuming that it indeed is correct, the radiologists stated that visualizing this contrast fluid would be a nice feature for inexperienced reviewers if the number of false positives can be reduced. The junior radiologist thought contrast visualization in general would be a nice addition but she did not think it would help find malignant lesions.

8. Conclusions

In this thesis we tried to enhance colon visualizations by either rearranging and emphasizing information that was already there, and/or by introducing new information that was not yet in the visualization with a main goal of increasing the number of lesions found or reducing the review time. We did this by using different reflection models, shadows and transparency techniques and by integrating lesion features in the visualization. The task for us at hand proved to be difficult. In the first two paragraphs we would like to answer the research questions we proposed in chapter 1.2. Next, we include some recommendations for future research and some final thoughts.

8.1. Feature-independent visualization

Our first research goal stated that we wanted to research whether it is possible to enhance the existing visualization without increasing the amount of visualized information. During the research towards this question we mainly focused on polyps because the shape information of flat lesions is quite unreliable or even absent.

Literature shows that experts are able find 90% of the polyps found with colonoscopy using CT colonography [Johnson et al. 2008]. The remaining 10% of the polyps is not found because the information describing these polyps is not present in the data, for example because they are surrounded by non-tagged stool. In short: Radiologists consider the problem of finding polyps solved. Furthermore, most radiologists use the orthogonal views as a primary reviewing method, the reason being that a lot more information can be perceived. Usually the 3D view is used when the reviewer is interested in the shape of a suspicious area, which is also the only thing he is interested in.

These factors make it very hard to enhance the existing visualization. It certainly would be possible to create a 3D visualization that approaches the level of information that is perceived using orthogonal views. However, this would not translate in an increased amount of found lesions or a reduced review time.

Our best attempts were the rim lighting technique as a non-feature based technique and the contrast visualizer that aids to reviewer to spot areas that have a thin film of contrast sticking to them. Although more information was visible using the rim light, in the experts opinions it did not help them with a

better understanding of what they saw. The contrast visualizer was seen as a nice feature but it does not provide them with the information they are looking for.

8.2. Feature dependent visualization

Our second research goal asked whether it would be possible to develop a techniques that increase the amount of information visualized thus giving the radiologist a better idea of what he is looking at. During this research the focus was mainly on flat lesions because these are considered to be the biggest problem.

It was obvious from the beginning that the problem of finding flat lesions would be a tough problem. This was backed up by the fact that even radiologists are unable to find 75% of the flat lesions in a CT scan (yet unpublished research by AMC). Unfortunately, the problem proved to be even harder than we thought. The features did not accurately describe the lesions. The deformed colon wall feature is a very unreliable feature. The raised HU value level proved to be not sufficiently high enough to be distinguishable. The only feature that could possibly be of value is the adhering contrast fluid. Although this feature is confirmed by our own findings, it has not been researched enough in order to give an definite answer. Another issue that proved to be a major problem with flat lesions is the lack of good data.

If the adhering contrast feature proves to be wrong, there is little left with which we can identify flat lesions. This translates to our results which were unacceptable. If the feature proves to be valid, results were acceptable. No flat lesion with adhering contrast were missed in the 21 data sets we tested, and false positives ranked between 3 and 30 areas per data set. Most false positives consisted of small pools of contrast that are easily identified as such. The rest is fecal residue. There is the danger that a polyp is dismissed as fecal residue when they are colored the same.

Experts assessed that the flat lesion coloring could help beginning reviewers improve their ratings if they used the 3D visualization as primary method. However it would also lengthen their reviewing times because of the false positives. Reviewers that use the orthogonal views as primary method would not benefit the coloring because they have already perceived the contrast information in the 2D views.

8.3. Further research

We performed a fairly broad investigation with many techniques that were tested. Although it can be theoretically argued that introducing new information in the 3D visualization will never be able to reach the level of information a 2D slice provides, the chance that 3D visualization might gain popularity is present.

We don't believe there is much to gain in the non-feature based visualizations. Some more ideas can be tested like interactive visualizations and glyph visualization. However, introducing new tools that reviewers will have to learn would only marginally increase the visualization while introducing a large increase in reviewing time as well. Moreover, if there is no obvious advantage the acceptance will be very low under radiologists. The only thing that is worth future investigations is the curvature visualization that might enhance the visualization in a subtle way, making it easier on the eye. The real advantage of this would have to be tested thoroughly because it is not likely to gain acceptance under radiologists if this advantage is not clearly present.

Some future research can be performed in the feature based visualization. Success will largely depend on the rate of acceptance under radiologists and the number of false positives, which in turn depends on the preparation of the patient. In our research we focused largely on the raised intensity and the adhering contrast fluid, which is clearly the best feature. However, it might be possible to combine this feature with the slightly elevated shape of the lesion, thereby ignoring its exact shape. Typical flat lesions are 6-10 mm and are protruding about 2-4 mm from the surface, which could possibly increase the confidence of the found candidates. In our results, a number of false positives were pools of contrast that clearly do not elevate from the surface.

Additionally we think that an objective evaluation might give a more decisive answer to the question whether 3D colon wall visualization as it is now can be enhanced. This would involve many radiologists and even more data sets, both of which are hard to come by. However we think such an evaluation would exclude any prejudices and would be beneficial. Radiologists have good reasons to be suspicious towards new technologies. Traditional techniques have been researched extensively, and radiologists have developed a feeling for these techniques. However, proof that it is possible to find as many or even more lesions with an enhanced visualization as with orthogonal slices only, might just be the final push that 3D visualization needs.

8.4. Final words

We cannot claim to have found a technique that substantially adds value to the current workflow of a typical radiologist, the reason being that the radiologist already has the means to find the information he wants. Part of the problem is the fact that the radiologists are still not ready to accept 3D visualization as their primary method. As a secondary method, 3D visualization is used by the radiologist to help him understand the shape of suspicious areas in orthogonal slices. Orthogonal slices show more information and do not necessarily need replacement.

We believe the flat lesion contrast visualization can be of assistance if the number of false positives is reduced to a maximum of 10 per colon scan which we believe can be done by incorporating the shape information.

This research has led to a decent understanding of why the current visualization techniques do their job well. We tried alternative techniques that seemed promising quite exhaustively. Also, we gained much more understanding of the behavior of flat lesions and their feasible features.

References

- [Amantides et al. 1987] Amantides, J. and Woo, A., “A fast voxel traversal algorithm for ray tracing”, Proceedings of Eurographics ‘87, 1987, pp 3-10
- [Bescós 2003] Bescós, J. O., “Isosurface Rendering”, University of Twente, 2003, Phd Thesis
- [Bosma 2000] Bosma, M., “Speed and Accuracy for Medical Applications”, Technical University Delft, 2000, Phd Thesis
- [O’Connor et al. 2006] O’Connor, S., Summers, R., Choi, J., and Pickhardt, P., “Oral contrast adherence to polyps on CT colonography.”, J Computer Assisted Tomography, volume 30, No. 1, 2006, pp 51-57
- [Cotton et al. 2004] Cotton, P. B., Durkalski, V. L., Pineau, B. C., Palesch, Y. Y., Mauldin, P. D., Hoffman, B., Vining, D. J., Small, W. C., Affronti, J., Rex, D., Kopecky, K. K., Ackerman, S., Burdick, J. S., Brewington, C., Turner, M. A., Zfass, A., Wright, A. R., Lyer, R. B., Lynch, P., Sivak, M. V., and Butler, H., “Computed Tomographic Colonography: A Multicenter Comparison With Standard Colonoscopy for Detection of Colorectal Neoplasia”, JAMA, volume 291, 2004, pp 1713-1719
- [Giardiello et al. 1995] Giardiello, F. M. and Offerhaus, J., “Phenotype and cancer risk of various polyposis syndromes.”, Eur J Cancer, volume 31A, No. 7-8, 1995, pp 1085-1087
- [Gonzalez et al. 2002] Gonzalez, R. C. and Woods, R. E., “Digital Image Processing”, Prentice Hall, 2002
- [Hawkes 2008] Hawkes, P. W., “Advances in Imaging and Electron Physics”, Academic Press, 2008
- [Hearn et al. 1997] Hearn, D. and Baker, M. P., “Computer Graphics”, Prentice Hall, 1997]
- [Hong et al. 2006] Hong, W., Gu, X., Qiu, F., Jin, M., and Kaufman, A., “Conformal Virtual Colon Flattening”, Proceedings of the 2006 ACM symposium on Solid and physical modeling, 2006, pp 85-93
- [Jarosz et al. 2008] Jarosz, W., henrik wann jensen, and craig donner, “Advanced Global Illumination Using Photon Mapping”, Siggraph, 2008,

- [Johnson et al. 2008] Johnson, C. D., Chen, M., Toledano, A. Y., and Heiken, J. P., “Accuracy of CT Colonography for Detection Accuracy of CT Colonography for Detection of Large Adenomas and Cancers”, *The New England Journal of Medicine*, volume 359, No. 12, 2008, pp 1207-1217
- [Kudo et al. 2000] Kudo, S., Kashida, H., and Tamura, T., “Colonoscopic diagnosis and management of nonpolypoid early colorectal cancer”, *World J Surg*, volume 24, No. 9, 2000, pp 1081-1090
- [Levoy 1988] Levoy, M. S., “Display of surfaces from volume data”, *IEEE Computer Graphics and Applications*, volume 8, No. 3, 1988, pp 28-37
- [Mishra et al. 2004] Mishra, R. K., Hanna, G. B., Brown, S. I., and Cuschieri, A., “Optimum shadow-casting illumination for endoscopic task performance”, *Arch Surg*, volume 139, No. 8, 2004, pp 889-892
- [Morimoto et al. 2002] Morimoto, L. M., Newcomb, P. A., Ulrich, C. M., Bostick, R. M., Lais, C. J., and Potter, J. D., “Risk factors for Hyperplastic and Adenomatous Polyps: Evidence for Malignant Potential?”, *Cancer Epidemiology Biomarkers & Prevention*, volume 11, 2002, pp 1012-1018
- [Neri et al. 2005] Neri, E., Vagli, P., Picchietti, S., Vannozzi, F., Linsalata, S., Bardine, A., and Bartolozzi, C., “CT colonography: contrast enhancement of benign and malignant colorectal lesions versus fecal residuals.”, *Abdominal Imaging*, volume 30, No. 6, 2005, pp 694-697
- [Park et al. 2007] Park, S. H., Lee, S. S., Choi, E. K., Kim, S. Y., Yang, S., Kim, J. H., and Ha, H. K., “Flat Colorectal Neoplasms: Definition, Importance and Visualization on CT Colonography”, *AJR Am J Roentgenol.*, volume 188, No. 4, 2007, pp 1953-9
- [Perlin 1985] Perlin, K., “An image synthesizer”, *ACM SIGGRAPH Computer Graphics*, volume 19, No 3, 1985,
- [Pickhardt et al. 2003] Pickhardt, P. J., Choi, J. R., Hwang, I., Butler, J. A., Puckett, M. L., Hildebrandt, H. A., Wong, R. K., Nugent, P. A., Mysliwiec, P. A., and Schindler, W. R., “Computed tomographic virtual colonoscopy to screen for colorectal neoplasia in asymptomatic adults”, *The New England Journal of Medicine*, volume 349, 2003, pp 2191-2200
- [Pickhardt 2004] Pickhardt, P. J., “Translucency Rendering in 3D Endoluminal CT Colonography”, *American Journal of Roentgenology*, volume 291, 2004, pp 1713-1719

- [Schaap et al. 2008] Schaap, M., Schilham, A. M. R., Zuiderveld, K. J., Prokop, M., Vonken, E. J., and Niessen, W. J., “Fast Noise Reduction in Computed Tomography for Improved 3-D Visualization”, IEEE Transactions on Medical Imaging, volume 27, No. 8, 2008, pp 1120-1129
- [Serlie 2007] Serlie, I., “Electronic Cleansing for Visualization in CT Colonography”, Technical University Delft, 2007, Phd Thesis
- [Shapiro 2002] L. Shapiro, G. Stockman, “Computer Vision”, Prentice hall, 69-73
- [Soetniko et al. 2008] Soetniko, R. M., Kaltenbach, T., and Rouse, R. V., “Prevalence of Nonpolypoid (Flat and Depressed) Colorectal Neoplasms in Asymptomatic and Symptomatic Adults”, JAMA, volume 299, No. 9, 2008, pp 1027-1035
- [Stryker et al. 1987] Stryker, S., Wolff, B., and Culp, C., “Natural history of untreated colonic polyps”, Gastroenterology, volume 93, No. 5, 1987, pp 1009-10013
- [Vilanova et al. 2001] Vilanova Bartrolí, A. V., Wegenkittl, R., König, A., and Gröller, E., “Nonlinear virtual colon unfolding”, VIS '01: Proceedings of the conference on Visualization '01, 2001, pp 411-420
- [Waye et al. 2003] Waye, J. D., Rex, D. K., and Williams, C. B., “Colonoscopy: Principles and Practice”, 2003,
- [Wijk et al. 2006] van Wijk, C., van Ravesteijn, V. F., Vos, F., Truyen, R., de Vries, A. H., Stoker, J., and van Vliet, L. J., “Detection of Protrusions in Curved Folded Surfaces Applied to Automated Polyp Detection in CT Colonography”, MICCAI, 2006, pp 471-478
- [Yoshida et al. 2002] Yoshida, H., Naepfi, J. J., Frimmel, H., and Dachman, A. H., “Computer-aided Diagnosis Scheme for Detection of Polyps at CT Colonography”, Proc. SPIE, volume 4684, 2002, pp 1235-1245
- [Zhao et al. 2006] Zhao, L., “Lines of Curvature for Polyp Detection in Virtual Colonoscopy”, IEEE Transactions on Visualization and Computer Graphics, volume 12, No. 5, 2006, pp 885-892

Additional references

[Bamboo 2006] Bamboo, G."Colon Polyps", Gold Bamboo, http://goldbamboo.com/topic-t3854-a1-6Colon_Polyps.html,

[Enders 2006] Enders, G. H. "Colonic Polyps ", WebMD, Emedicine, <http://www.emedicine.com/med/topic414.htm>, August 6th, 2008

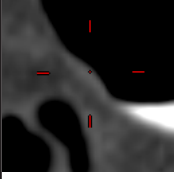
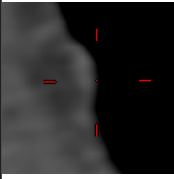
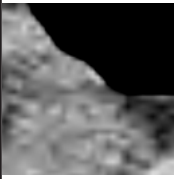
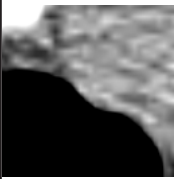
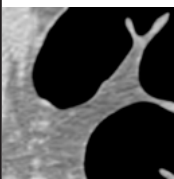
[Medcyclopaedia 2008] Medcyclopaedia "Hounsfield units", Medcyclopaedia, http://www.medcyclopaedia.com/library/topics/volume_iii_1/h/hounsfield_unit.aspx,

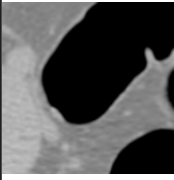


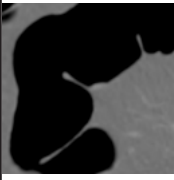
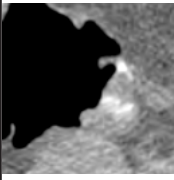
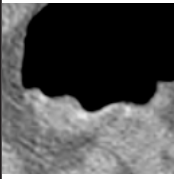
[Santoro et al. 2008] Santoro, M. and Lee, D. "Colon polyps", Medicine Net, http://www.medicinenet.com/colon_polyps/article.htm, August 7th, 2008

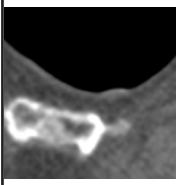
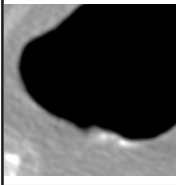
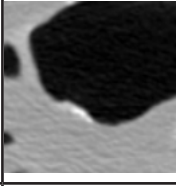
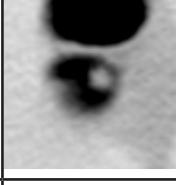
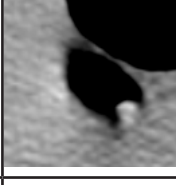
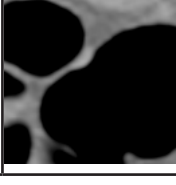
[Charette 2008] Charette, A."Colon polyps", UpToDate for Patients, <http://www.uptodate.com/patients/content/topic.do?topicKey=digestiv/9798>

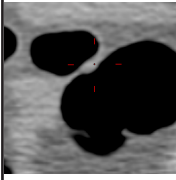
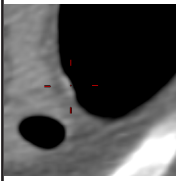
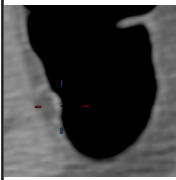

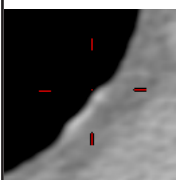
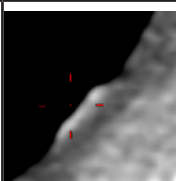
Appendix A: Flat lesion index

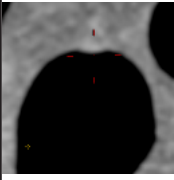
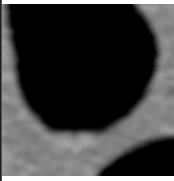
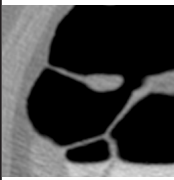
In order to develop a decent understanding of the appearance of flat lesions we developed the following index of 25 flat lesions in 14 patients. Highest HU value refers to the highest value in the flat lesion, which might indicate that contrast fluid sticks to the surface. Part of Cluster refers to the question whether nearby organs or fluid pools make it hard to distinguish the lesion. Adhering contrast is mainly based on the highest HU value and determines whether contrast adheres to the lesion. The cluster size is found by thresholding the data at 100 HU and performing a connected component analysis. The data has been published with permission of AMC.

| Patient id | Suppine/ prone | Number of slices | Diameter in mm | Location | Voxel location (x,y,z) | Highest HU value | Part of cluster | Adhering contrast | Cluster size > 100 HU | |
|------------|-------------------|---------------------|-------------------|------------|---------------------------|---------------------|-----------------|----------------------|--------------------------|---|
| 1 | Prone | 451 | 6 | Transverse | 255,155,315 | 130 | Fluid close | Yes | 3 |  |
| 1 | Suppine | 467 | 6 | Transverse | 223,341,295 | 95 | Yes | Slightly | 0 |  |
| 2 | Suppine | 465 | 6 | Sigmoid | 213,258,185 | 96 | Yes | No | 0 |  |
| 2 | Prone | 470 | 6 | Sigmoid | 300,284,183 | 112 | Yes | No | 36 |  |
| 3 | Prone | 469 | 6 | Sigmoid | 309,281,120 | 132 | No | Yes | 14 |  |

| Patient id | Suppine/ prone | Number of slices | Diameter in mm | Location | Voxel location (x,y,z) | Highest HU value | Part of cluster | Adhering contrast | Cluster size > 100 HU | |
|------------|-------------------|---------------------|-------------------|------------|---------------------------|---------------------|-----------------|----------------------|--------------------------|---|
| 3 | Suppine | 469 | 6 | Sigmoid | 188,248,129 | 181 | No | Slightly | 4 |  |
| 4 | Prone | 448 | 8 | Descending | 76,290,294 | 231 | No | Yes | 40 |  |
| 4 | Suppine | 422 | 8 | Descending | 432,203,282 | 285 | No | Yes | 67 |  |
| 5 | Suppine | 492 | 8 | Transverse | 197,191,345 | -4 | No | Slightly | 0 |  |
| 6 | Prone | 494 | 45 | Caecum | 290,290,198 | 304 | N/A | Yes | 8204 |  |
| 6 | Supine | 494 | 45 | Caecum | 163,226,171 | 231 | N/A | Yes | 9451 |  |

| Patient id | Suppine/ prone | Number of slices | Diameter in mm | Location | Voxel location (x,y,z) | Highest HU value | Part of cluster | Adhering contrast | Cluster size > 100 HU | |
|------------|-------------------|---------------------|-------------------|-----------|---------------------------|---------------------|-----------------|----------------------|--------------------------|---|
| 7 | Prone | 436 | 7 | Rectum | 256,169,86 | 174 | No | Yes | 10 |  |
| 8 | Prone | 462 | 12 | Ascending | 366,300,205 | 539 | No | Yes | 322 |  |
| 8 | Suppine | 463 | 12 | Ascending | 142,226,184 | 376 | No | Yes | 345 |  |
| 9 | Prone | 498 | 7 | Hepatic | 341,253,404 | 115 | Yes | Yes | 8 |  |
| 9 | Suppine | 500 | 7 | Hepatic | 196,254,401 | 198 | Slightly | Yes | 73 |  |
| 10 | Suppine | 417 | 6 | Sigmoid | 302,176,120 | 116 | Slightly | Slightly | 3 |  |

| Patient id | Suppine/ prone | Number of slices | Diameter in mm | Location | Voxel location (x,y,z) | Highest HU value | Part of cluster | Adhering contrast | Cluster size > 100 HU | |
|------------|-------------------|---------------------|-------------------|------------|---------------------------|---------------------|-----------------|----------------------|--------------------------|---|
| 10 | Prone | 409 | 6 | Sigmoid | 216,362,119 | 98 | Slightly | Slightly | 0 |  |
| 11 | Prone | 390 | 6 | Descending | 129,259,169 | 144 | No | Yes | 7 |  |
| 11 | Suppine | 379 | 6 | Descending | 391,248,180 | 104 | Yes | Slightly | 6 |  |
| 12 | Suppine | 232 | 20 | Ascending | 184,153,65 | 265 | Yes | Slightly | 40 |  |
| 13 | Suppine | 808 | 7.7 | Rectum | 278,360,201 | 199 | No | Slightly | 52 |  |
| 13 | Prone | 827 | 7.7 | Rectum | 300,208,660 | 161 | No | Slightly | 13+13 |  |

| Patient id | Suppine/ prone | Number of slices | Diameter in mm | Location | Voxel location (x,y,z) | Highest HU value | Part of cluster | Adhering contrast | Cluster size > 100 HU | |
|------------|-------------------|---------------------|-------------------|----------|---------------------------|---------------------|-----------------|----------------------|--------------------------|---|
| 14 | Suppine | 853 | 7.4 | Sigmoid | 229,237,339 | 7 | Yes | No | 0 |  |
| 14 | Prone | 870 | 4.3 | Sigmoid | 202,296,562 | 18 | Yes | No | 0 |  |
| 15 | Suppine | 482 | 10 | Caecum | 128,239,280 | 27 | Yes | No | 0 |  |

